Agricultural Water Management 278 (2023) 108142

Contents lists available at ScienceDirect

Agricultural Water Management

journal homepage: www.elsevier.com/locate/agwat

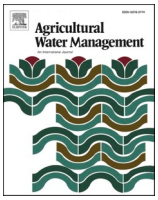

Assessment of agricultural drought based on multi-source remote sensing data in a major grain producing area of Northwest China

Siyang Cai [a], Depeng Zuo [a,*], Huixiao Wang [a,*], Zongxue Xu [a], GuoQing Wang [b], Hong Yang [c]

[a] College of Water Sciences, Beijing Key Laboratory of Urban Hydrological Cycle and Sponge City Technology, Beijing Normal University, Beijing 100875, China
[b] Nanjing Hydraulic Research Institute, Nanjing 210029, Jiangsu, China
[c] Eawag, Swiss Federal Institute of Aquatic Science and Technology, P.O. Box 611, 8600 Dübendorf, Switzerland

ARTICLE INFO

Handling Editor - Dr R Thompson

Keywords:
Agricultural drought
Scaled Drought Condition Index
Multi-drought indices
Crop yield
Drought disaster

ABSTRACT

Drought is considered to be one of the most serious natural disasters in China, which can result in enormous damage to nature and socio-economy. Compared to traditional ground-based monitoring techniques, remote sensing can effectively compensate for spatial discontinuities at ground stations. The use of remote sensing technology for drought monitoring has irreplaceable advantages. The applicability of the TRMM3B43 dataset for precipitation was firstly verified in the Wei River basin, and the spatiotemporal characteristics of precipitation were analyzed. Based on the TRMM3B43, MODIS NDVI, and MODIS LST datasets, the spatiotemporal variations of drought were secondly investigated by calculating the Precipitation Condition Index (PCI), Vegetation Condition Index (VCI), and Temporal Condition Index (TCI). Crop yield was employed as the reference of drought impact for evaluating the applicability of the Scaled Drought Condition Index (SDCI) based on the combination of the PCI, VCI, and VCI by four kinds of weight determination methods, i.e. Analytic Hierarchy Process (AHP), Entropy method, Criteria Importance Through Intercriteria Correlation (CRITIC), and Fuzzy Comprehensive Evaluation (FCE). Finally, the agricultural drought calculated by the SDCI was evaluated against drought area, disaster area, and crop failure area to verify the applicability of the SDCI for agricultural drought disaster assessment in the Wei River basin. The results showed that the SDCI determined by FCE has better correlations with crop yield (R^2 =0.45) than the other methods. The SDCI values exhibited a "W" shape from 2003 to 2010 during the growing seasons and agricultural drought showed an increasing trend after 2013. The drought-prone areas shifted from north to south, with the degree of drought firstly decreasing and then increasing. In addition, the SDCI has better correlations with the disaster area (R^2 =0.35) than the drought area (R^2 = 0.16). At the municipal level, the SDCI could well assess agricultural drought. The results demonstrated that the SDCI can effectively monitor and assess drought impacts on agriculture and may provide helpful information for agricultural drought disaster prevention.

1. Introduction

Drought is a progressive and recurrent natural disaster that occurs almost everywhere in the world, making it one of the most devastating natural disasters (Schubert et al., 2016; Yao et al., 2018). Drought deeply affects the ecological and socio-economic sectors (Zhong et al., 2019). Drought and extreme heat are responsible for 9%–10% of the decline in national cereal production (Lesk et al., 2016). The drought negatively affected different sectors of the Netherlands, resulting in an estimated damage of 450–2080 million Euros in the summer of 2018 (Sjoukje et al., 2020). According to data issued by the Bulletin of food and drought disaster in China, China's annual drought losses due to agricultural disasters are 16.302 billion kilograms, accounting for more than 60% of all kinds of natural disasters that caused grain losses between 1950 and 2016 (Zhang et al., 2019). The development of drought monitoring and assessment methods has attracted the interest of many researchers as drought events become more frequent and severe on a global scale (Hu et al., 2019).

Drought indices can effectively monitor drought based on in-situ observations. Based on water supply and demand, Palmer (1965) came up with a drought index-the Palmer Drought Index (PDSI), which means that the local area is considered as dry when its water supply is

* Corresponding authors.
E-mail addresses: dpzuo@bnu.edu.cn (D. Zuo), huixiaowang@bnu.edu.cn (H. Wang).

https://doi.org/10.1016/j.agwat.2023.108142
Received 24 October 2022; Received in revised form 16 December 2022; Accepted 3 January 2023
Available online 9 January 2023

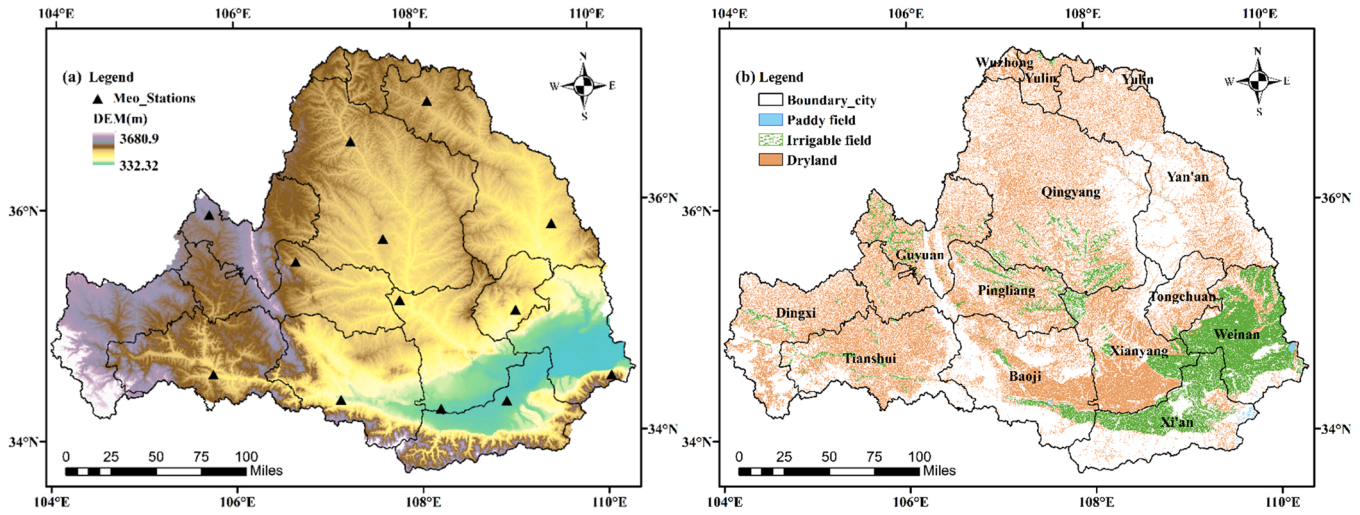

Fig. 1. (a) Digital elevation model and location of meteorological stations; (b)Spatial distribution of land cover of 2005 in the Wei River basin of China.

less than its demand, and wet otherwise. The PDSI considers not only the current water supply and demand but also the impact of previous wet and dry conditions and their duration on the current drought conditions. To address regional differences in parameters and improve the portability and spatial comparability of the PDSI, Wells et al. (2004) proposed an adaptive PDSI (self-calibrating PDSI, scPDSI), that can be automatically corrected for the local climate. Mckee et al. (1993) proposed the Standardized Precipitation Index (SPI), which is a cumulative probability function derived from successive time series of precipitation at a time scale and allowed for comparisons over multiple time scales, reflecting not only changes in precipitation but also the evolution of water resources over a period. The Standardized Precipitation Evapotranspiration Index (SPEI) was developed by Vicente-Serrano et al. (2010), which considered both precipitation and potential evapotranspiration in determining drought as an extension of the widely used SPI (Beguería et al., 2014). The above three drought indicators are currently the most widely used indicators to assess drought events (Trenberth et al., 2014; Chen and Sun, 2015; Wang et al., 2016).

Ground-based observations or interpolated grids were widely used to monitor and investigate drought in the past (Hayes et al., 1999; Sheffield et al., 2012). The dataset based on observation could not effective in capturing drought-related characteristics in agriculture at a regional scale. At present, Remote Sensing technology has the advantages of wide coverage, strong data continuity, objectivity, and timeliness, making it the most promising technology in drought monitoring., a series of indices have been developed which overcome the shortcoming of spatial monitoring ability of in-situ indices (Sur et al., 2015; Park et al., 2017; Xu et al., 2018). Normalized Difference Vegetation Index (NDVI) (Kogan, 1995a), Land Surface Temperature (LST) (Kogan, 1995a), Vegetation Condition Index (VCI) (Kogan, 1995b), Temperature Condition Index (TCI) (Kogan, 1995a), Soil Moisture Condition Index (SMCI) (Zhang and Jia, 2013) and other related indices based on remote-sensing data have been widely used to monitor and assess agricultural drought worldwide. With the increase of remote sensing satellites, the quality of remote sensing data is constantly improving, providing a rich source of information for drought monitoring using multi-source remote sensing data (Aghakouchak et al., 2015; Kalisa et al., 2020).

Factors contributing to drought include the regional climate (precipitation, temperature) and local surface characteristics (land cover, vegetation community) (Barker et al., 2015; Van Loon and Laaha, 2015). Relying on single factor based drought index cannot accurately monitor and evaluate drought events, therefore, various combination drought indices are proposed to monitor drought conditions by combining a single remote sensing drought indices. Based on the TCI, PCI, and SMCI indices, Zhang and Jia (2013) proposed the microwave integrated drought index (MIDI), which is used to monitor short-term droughts, especially meteorological droughts in North China. Sánchez et al. (2016) developed the Soil Moisture Agricultural Drought Index (SMADI) combines SMOS-SSM and MODIS-derived LST while including the 8 days lagged response of MODIS NDVI for the whole Iberian Peninsula. Zuo et al. (2019) structured the Combined Deficit Index (CDI) based on precipitation and NDVI from the two sources of data under dryland to assess the agricultural drought in Northeast China. The Vegetation Supply Water Index (VSWI) based on NDVI and LST was aimed at capturing changes in soil moisture in crops to determine whether the crop was experiencing drought even if crops were not significantly dry (Chen et al., 2020a; Fazi et al., 2020). Liu et al. (2020) analyzed drought using a combination of PCI, VCI, SMCI, and TCI and found that MCDI-1 and MCDI-9 were suitable for meteorological drought monitoring and agricultural drought monitoring, respectively in Shandong of China. Wu et al. (2021) proposed univariate soil moisture and evapotranspiration index (USMEI) and bivariate soil moisture and evapotranspiration index (BSMEI) based on evapotranspiration and soil moisture to reflect water stress for winter wheat in the North China Plain.

The Wei River, the largest tributary of the Yellow River, is a climate-sensitive area in China where drought disasters frequently occurred due to the uneven distribution of precipitation in spatial and temporal domain (Zhu et al., 2017). Agricultural land accounts for about 60% of the total basin area, and drought causes more than 50% of the total agricultural losses (Yuan et al., 2016; Ding et al., 2019). Therefore, the comprehensive study on the evolution characteristics of drought in the Wei River basin is of great significance to the sustainable development of social economy. At present, the researches in the Wei River basin involve meteorological drought assessment (Huang et al., 2014; Zhao et al., 2020), hydrological drought monitoring (Lai et al., 2019; Jehanzaib et al., 2020), and its response to meteorological drought (Huang et al., 2017; Fang et al., 2020; Guo et al., 2020). In addition, Yang et al. (2018) and Zhang et al. (2019) developed a multivariate standardized drought index based on precipitation (meteorology), runoff (hydrology), and soil moisture (agriculture) information for drought monitoring and risk assessments. Therefore, the assessment of agricultural drought based on multi-source remote sensing data in the Wei River basin, a major grain producing area of Northwest China, has great scientific significance for agricultural drought disaster prevention and agricultural water management.

In this study, the Scaled Drought Condition Index (SDCI) was firstly developed for agricultural drought assessment which is calculated based

Table 1
Datasets used in this study.

Group	Dataset	Description	Resolution	Period
SDCI inputs	TRMM	Tropical Rainfall Measuring Mission	0.25°-Monthly	2000–2016
	MODIS13A2 (NDVI)	Moderate resolution imaging spectroradiometer product 13A2	1 km-16 day	2000–2016
	MODIS11A2 (LST)	Moderate resolution imaging spectroradiometer product 11A2	1 km-8 day	2000–2016
SDCI validation	Crop yield	Crop yield of winter wheat and corn, rice, and so on in the Wei River basin	Regional-yearly	2000–2016
	Sown area	Area sown or transplanted with crops	Regional-yearly	2001–2016
	Drought area	Areas where crop yield have been reduced by more than 10% due to drought	Regional-yearly	2000–2016
	Disaster area	Areas where crop yield have been reduced by more than 30% due to drought	Regional-yearly	2000–2016
	Crop failure area	Areas where crop yield have been reduced by more than 80% due to drought	Regional-yearly	2000–2016

Table 2
Datasets description on crop production.

Name	Region	Period	Missing data
Sown area	Gansu Province	2001–2016	/
	Shaanxi Province		
Drought area	Gansu Province	2000–2016	2002、2009、
	Shaanxi Province	2000–2016	2010
			/
Disaster area	Gansu Province	2000–2016	2008
Crop failure area	Shaanxi Province	2000–2016	2002、2008

Table 3
Classification of drought calculated by the Scaled Drought Condition Index.

Categories of drought	PCI	TCI	VCI	SDCI
Exceptional Drought	0–0.1	0–0.1	0–0.1	0–0.1
Extreme Drought	0.1–0.2	0.1–0.2	0.1–0.2	0.1–0.2
Severe Drought	0.2–0.3	0.2–0.3	0.2–0.3	0.2–0.3
Moderate Drought	0.3–0.4	0.3–0.4	0.3–0.4	0.3–0.4
Slight Dry	0.4–0.5	0.4–0.5	0.4–0.5	0.4–0.5
No Drought	0.5–1.0	0.5–1.0	0.5–1.0	0.5–1.0

on Precipitation Condition Index (PCI), Vegetation Condition Index (VCI), and Temperature Condition Index (TCI) using TRMM and MODIS dataset; then, crop yield was employed as the reference of drought impact for evaluating the applicability of the SDCI with four kinds of weight determination methods during the growing seasons from 2000 to 2016; finally, the drought area, disaster area, and crop failure area were used to validate the accuracy of the SDCI for assessing drought disaster. The main objectives are as follows: (1) to verify the applicability of TRMM data in the Wei River basin; (2) to identify the spatiotemporal pattern of droughts condition based on PCI, VCI, and TCI; (3) to determine the optimal weights for the SDCI using four optimization methods; (4) to investigate and evaluate agricultural drought calculated by the SDCI; (5) to validate the SDCI against agricultural crop production, including drought area, disaster area, and crop failure area.

2. Materials and methods

2.1. Study area

The Wei River is the largest tributary of the Yellow River, originating from Niaoshu Mountain in Weiyuan County of Gansu Province, flowing across Gansu Province, Ningxia Hui Autonomous Region, and Shaanxi Province, and merging into the Yellow River at Tongguan, Shaanxi Province in the lower reaches (Fig. 1(a)). The Wei River basin (WRB) locates between latitude 33°50 N and 37°18 N and longitude 104°E and 110°20′E, with a total length of 818 km and a total area of 1.348×10^5 km^2. For the development of the New Silk Road under the Belt and Road Initiative, the WRB is located in an important position, as well as an important grain production base in China (Li et al., 2015, 2017b; Zhao et al., 2015; Zhang et al., 2021).

The WRB is a temperate continental monsoon climate with hot summers and cold winters. Precipitation is concentrated in the summer months, with more than 60% of the annual average precipitation occurring from July to September (Gao et al., 2012). The average annual precipitation in the WRB is 572 mm, and the evaporation from the water surface is 660–1200 mm, decreasing from east to west and from north to south. The average annual temperature is in the range of 7.8 ~ 13.5 °C, and the average temperature increases from west to east. The annual sunshine hours range from 1900 to 2600 h. Decreasing precipitation and runoff have led to an imbalance between water supply and demand (Huang et al., 2014, 2017b; Liu et al., 2018), resulting in frequent drought disasters in the WRB (Yang et al., 2018).

The WRB has a resident population of 40.92×10^6, a crop sown area of 38.53×10^5 hectares, a crop production of 15.69×10^5 tons, and a regional GDP of 20.74×10^7 yuan in 2019. Compared with floods, wind hail, and other meteorological disasters, drought areas and crop failure areas of crops by drought accounted for about 68% of the total drought areas and crop failure areas of crops with 10.92×10^5 hectares and 12.93×10^4 hectares in 2017, respectively, which are reported by National Cryosphere Desert Data Center. The WRB is a relatively developed area in northwest China and one of the important grain, cotton, and oil producing areas and industrial production bases in China. Therefore, the stable and high yield of agriculture in this region is of great importance to the food security of western China and even the whole country.

2.2. Data description

The datasets used in this study are divided into two categories: 1) input datasets used for establishing SDCI, including TRMM, NDVI, and LST data; and 2) datasets used for validating the SDCI, including crop yield, sown area, drought area, disaster area, and crop failure area. Details of these datasets are shown in Table 1.

2.2.1. Meteorological gauging data

The meteorological data were obtained from the monthly rainfall data of 13 meteorological stations of the National Meteorological Science Data Center from 2000 to 2016 (http://www.nmic.cn/). The location of the 13 meteorological stations were shown in Fig. 1(a).

2.2.2. TRMM data

The Tropical Rainfall Measuring Mission (TRMM) dataset is used from the TRMM satellite jointly developed by the National Aeronautics and Space Administration (NASA) and Japan's National Space Development Agency (NASDA) (https://daac.gsfc.nasa.gov/datasets). The TRMM 3B43 dataset was selected with a spatial resolution of 0.25° × 0.25° from 2000 to 2016 and is given as the monthly interval. The dataset records the rate of precipitation given in mm/h, which need to be multiplied by the total number of hours in the corresponding month to obtain monthly precipitation data in mm.

At present, TRMM data was widely used in the field of drought assessment in various countries (Zhao and Yatagai, 2014; Sahoo et al.,

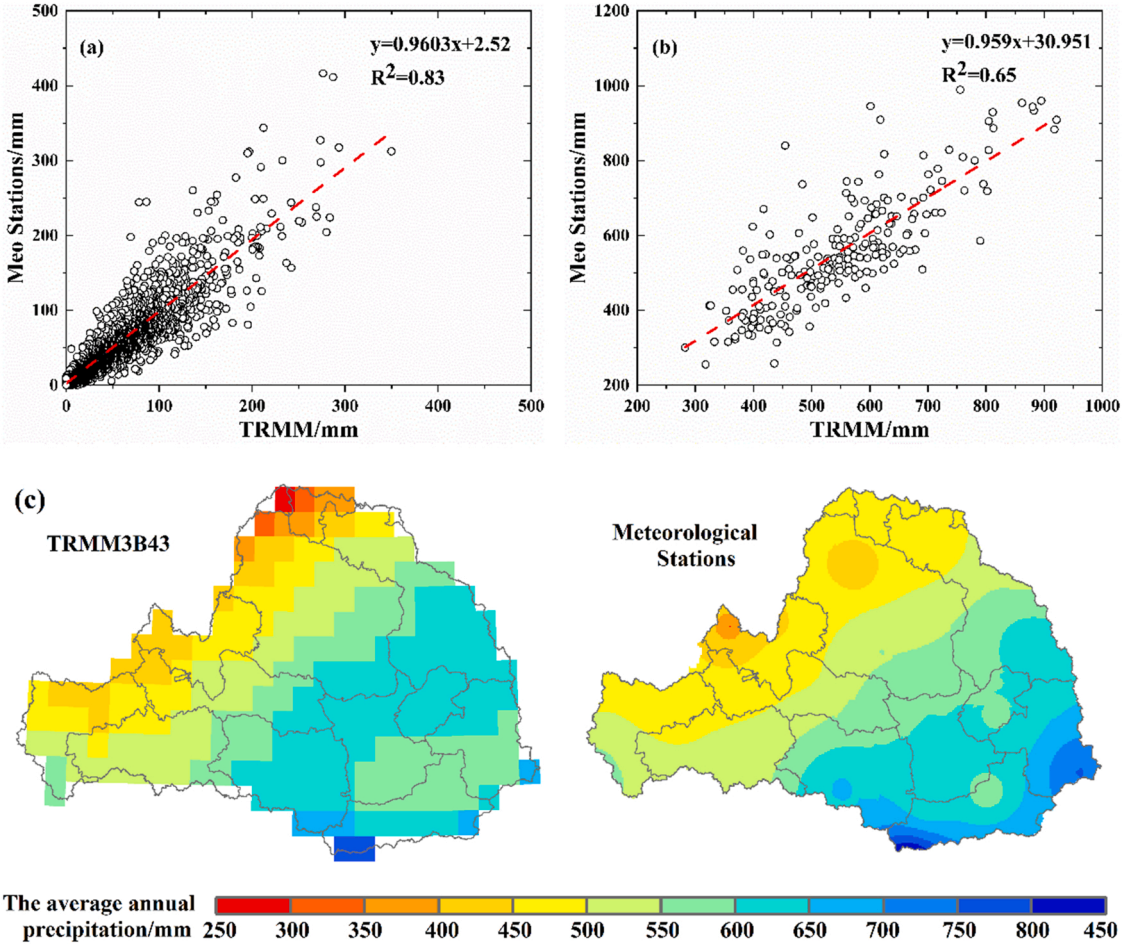

Fig. 2. Comparison of the temporal and spatial distribution of TRMM3B43 and 13 meteorological stations. (a)at the monthly scale; (b)at the yearly scale; (c)spatial distribution difference of multi-year average precipitation.

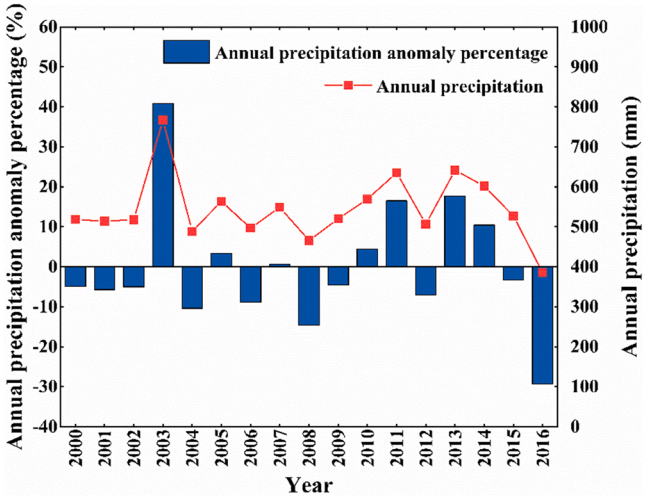

Fig. 3. The variation of annual precipitation and annual precipitation anomaly percentage based on TRMM3B43 in the Wei River basin during the period 2000–2016.

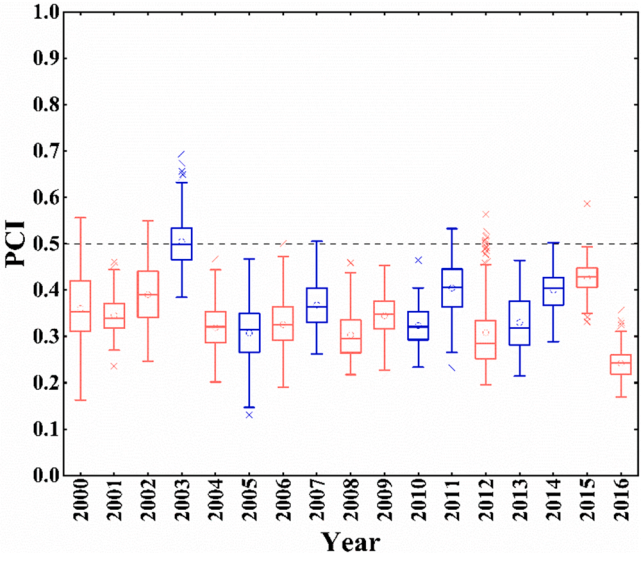

Fig. 4. Comparisons of the Precipitation Condition Index based on the TRMM3B43 dataset in the Wei River basin for the period 2000–2016. (The dot and lines indicate the mean value, 25th percentile, 50th percentile, and 75th percentile; the upper and lower horizontal lines outside of the box are the largest and smallest values; the outliers are shown as crosses).

2015; Cruz-Roa et al., 2017; Guo et al., 2019). However, there were few analysis of the applicability of the TRMM dataset in the WRB. Therefore, rainfall from the selected 13 in-situ stations was compared with TRMM 3B43 at the corresponding grid from 2000 to 2016 for accuracy

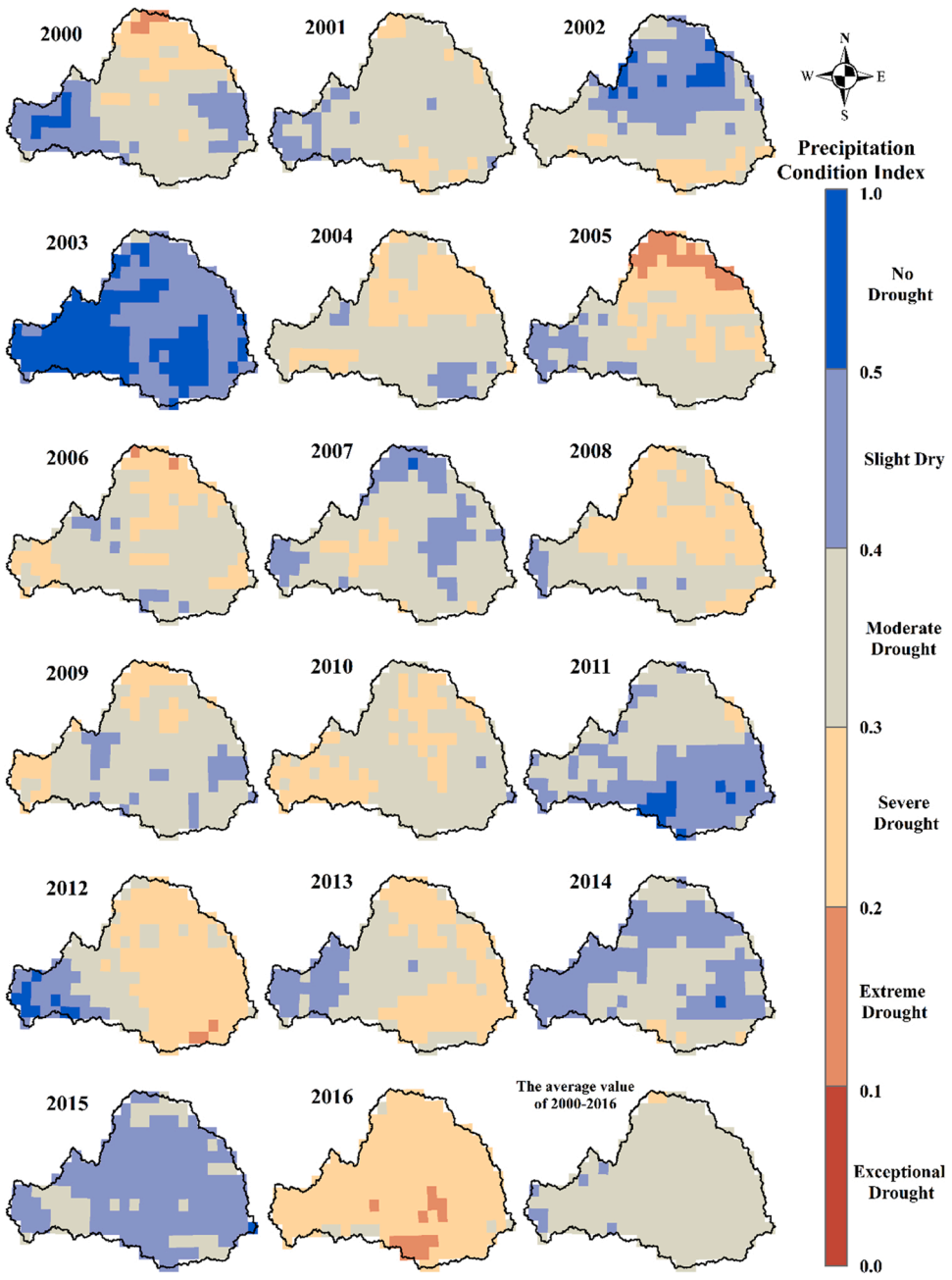

Fig. 5. Spatial distribution of the Precipitation Condition Index in the Wei River basin during the period 2000–2016.

verification at annual and monthly time scales in the following analysis.

2.2.3. MODIS data

The MODIS/Terra products used in the study are MODIS 11A2 (Land Surface Temperature, LST) and MODIS 13A2 (Normalized Differential Vegetation Index, (NDVI) were downloaded from https://modis.gsfc.nasa.gov/, both with a spatial resolution of 1 km and temporal interval of 8-day and 16-day, respectively. Monthly TCI and VCI were calculated using LST and NDVI from 2000 to 2016. The numbers h26v05 and h27v05 cover the study area.

2.2.4. Land cover data

The National Earth System Science Data Sharing Infrastructure of China offers land cover data (http://www.geodata.cn/), there are two main categories of the dataset. The dataset covers 6 primary types of forest, grassland, farmland, settlement, wetlands and water bodies, desert, and 25 secondary types. The secondary type of farmland is divided into paddy field, irrigable land, and dryland. The study used the land cover dataset for 2005 with a spatial resolution of 100 × 100 m and the land cover of the Wei River basin is shown in Fig. 1(b).

2.2.5. Crop yield data

The WRB covers Gansu Province, Ningxia Hui Autonomous Region, and Shaanxi Province. Gansu Province includes Tianshui, Pingliang, Qingyang, and Dingxi Cities; Ningxia Hui Autonomous Region includes Guyuan and Wuzhong Cities; Shaanxi Province includes Xi'an, Tongchuan, Baoji, Xianyang, Weinan, Yan'an and Yulin Cities. Among them, the data of crop yield (CY) for Gansu Province, Shaanxi Province and Ningxia Hui Autonomous Region are provided by Gansu Statistical Yearbook, Shaanxi Statistical Yearbook and Ningxia Statistical Yearbook during the period 2000–2016, respectively. The yield per hectare of Shaanxi Province during the period 2001–2016 was also obtained from

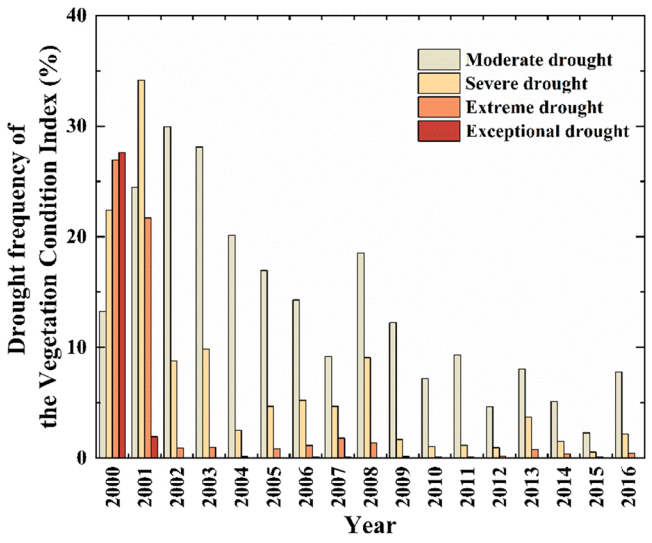

Fig. 6. Drought frequency of the Vegetation Condition Index in the Wei River basin during the period 2000–2016.

Shaanxi Statistical Yearbook. The statistical yearbook of three province were downloaded from National Bureau of Statistics (https://data.stats.gov.cn/).

2.2.6. Drought disaster data

Winter wheat, corn, sorghum, soybean, and rice are the main crop types in the WRB. Due to the proportion of corn being greater than that of winter wheat in the WRB, therefore, corn was selected as typical crop for the applicability analysis of drought indices. In addition, the corn's growing period (June – September) was determined as growing season in this study.

Due to the availability of data, the sown area includes Gansu Provinces and Shaanxi provinces and excludes Ningxia Hui Autonomous Region from 2001 to 2016. The drought area, disaster area, and crop failure area are statistical data of summer and autumn crops caused by drought, and it is impossible to distinguish the impact of drought on the two types of crops. Therefore, the data of drought disaster could verify the applicability of the SDCI in the study area to a certain extent. The sources of all disaster data are consistent with that of crop yield data. Details regarding these datasets are listed in Table 2.

2.2.7. Agricultural modernization

The Total Agricultural Machinery Power refers to total mechanical power of machinery used in agriculture, forestry, animal husbandry and fishery, including machinery for ploughing, irrigation and drainage, harvesting, transport, plant protection, and so on. The Consumption of Chemical Fertilizers in Agriculture refers to the quantity of chemical fertilizers applied in agriculture in a year, including nitrogenous fertilizer, phosphate fertilizer, potash fertilizer, and compound fertilizer. The consumption of chemical fertilizers is calculated in terms of amount of effective components by means of converting the gross weight of the respective fertilizers into weight containing effective component (such as nitrogen content in nitrogenous fertilizer, phosphorous pentoxide contents in phosphate fertilizer, and potassium oxide contents in potash fertilizer). The data of Total Power of Agricultural Machinery and Consumption of Chemical Fertilizers in Agricultural of Shaanxi Province during the period 2000–2016 were obtained from Shaanxi Statistical Yearbook.

2.3. Methods

2.3.1. Calculations of drought indices

2.3.1.1. The Precipitation Condition Index. Previous studies have shown that NDVI does not respond immediately after precipitation, and agricultural drought generally has a lag time of 3 months (Potop et al., 2015; Wu et al., 2016). Huang et al. (2015) proved that the lag time in summer is approximately 3 months in the WRB. Therefore, the cumulative precipitation for previous three months is used to characterize the precipitation condition for the current month. For instance, the amount of precipitation in June is the sum of precipitation in April, May, and June. Furthermore, the monthly PCI is calculated by the following equation:

$$\mathrm{PCI} = \frac{\mathrm{PCI_j} - \mathrm{PCI_{min}}}{\mathrm{PCI_{max}} - \mathrm{PCI_{min}}}$$

where PCI_{min} and PCI_{max} are the minimum and maximum values of PCI at each grid in i month; PCI_j represents the precipitation in i month during the period 2000–2016.

2.3.1.2. The Vegetation Condition Index. In recent years, Normalized Differential Vegetation Index (NDVI) is not only used to reflect the growth of vegetation but also used to assess drought events by many scholars (Park et al., 2016; Gazol et al., 2018; Chu et al., 2019).

However, the growing seasons of crops in different regions are in respective stages with different water conditions, therefore, the dry/wet condition of crops cannot be explained only by the values of NDVI. Kogan (1995b) proposed the Vegetation Condition Index, and its calculation formula is as follows:

$$\mathrm{VCI_j} = \frac{\mathrm{NDVI_j} - \mathrm{NDVI_{min}}}{\mathrm{NDVI_{max}} - \mathrm{NDVI_{min}}}$$

where $NDVI_j$ is the smoothed monthly NDVI; $NDVI_{max}$ and $NDVI_{min}$ represent maximum and minimum *NDVI*, respectively, calculated by multiyear smoothed monthly NDVI series for each pixel during the period 2000–2016.

2.3.1.3. The Temperature Condition Index. The land surface temperature (LST) is strongly associated with drought, and the temperature rise is the initial indication of the crops being treated with moisture stress and drought. The increase of temperature and the closure of leaf stomata can reduce the water loss caused by transpiration, reduce the surface latent heat flux, increase the surface sensible heat flux, and then cause the increase of temperature. Based on this principle, Kogan (1995a) proposed the Temperature Condition Index (TCI), and its calculation formula is as follows:

$$TCI_j = \frac{\mathrm{LST_{max}} - \mathrm{LST}_j}{\mathrm{LST_{max}} - \mathrm{LST_{min}}}$$

where LST_j is the smoothed monthly *LST*; LST_{max} and LST_{min} represent maximum and minimum *LST*, respectively, calculated by multiyear smoothed monthly LST series for each pixel during the period 2000–2016.

2.3.1.4. The Scaled Drought Condition Index. Rhee et al. (2010) proposed an agricultural drought index (Scaled Drought Condition Index, SDCI) based on VI, LST and TRMM that can assess drought conditions well in both dry and humid areas. And its calculation formula is as follows:

$$\mathrm{SDCI} = \alpha * \mathrm{VCI} + \beta * \mathrm{TCI} + \gamma * \mathrm{PCI}$$

where α、β and γ are the weights of monthly VCI、TCI and PCI, respectively, and $\alpha + \beta + \gamma = 1$.

Table 3 shows the drought classification by the PCI, TCI, VCI, and

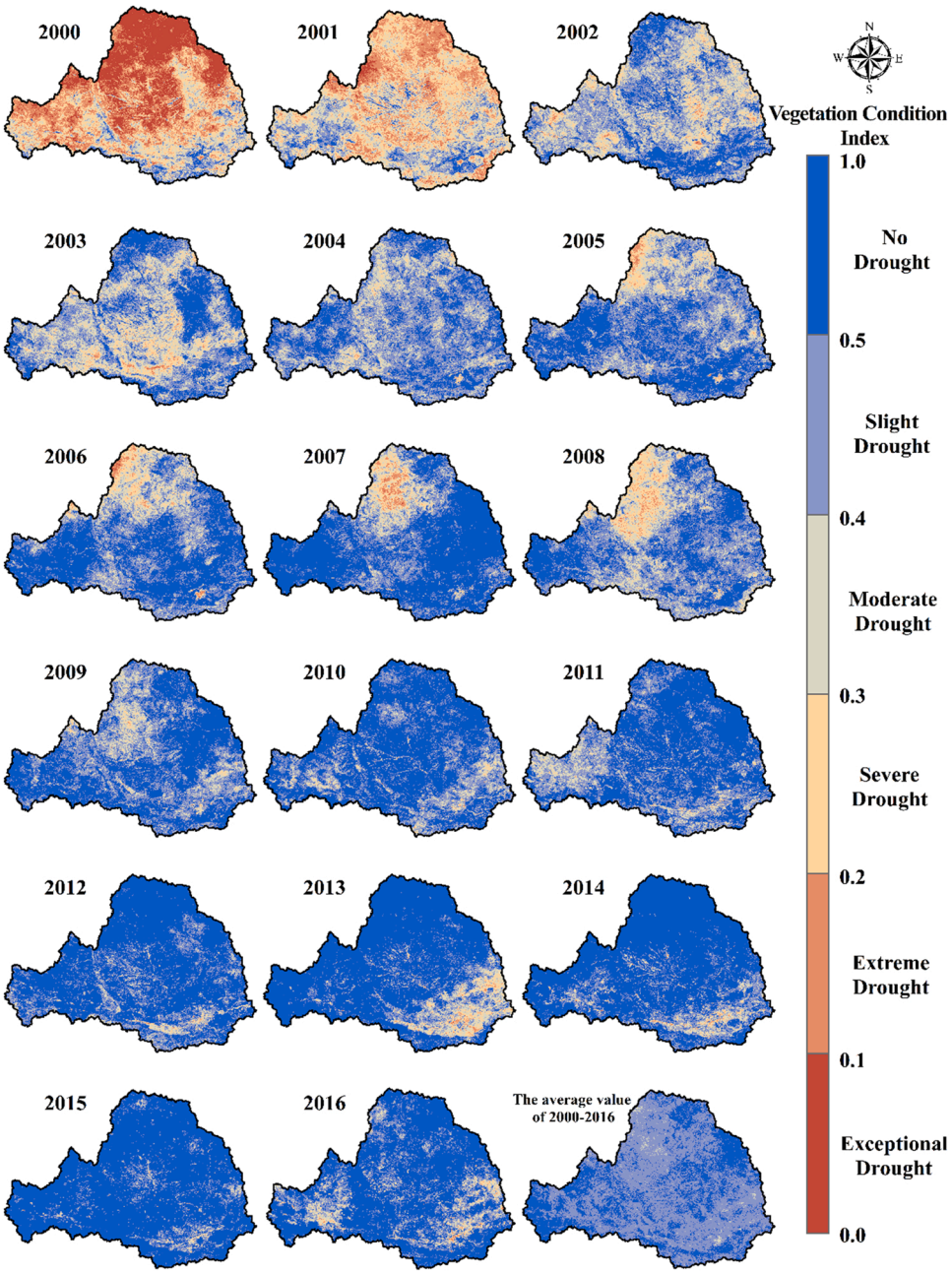

Fig. 7. Spatial distribution of the Vegetation Condition Index in the Wei River basin during the period 2000–2016.

SDCI.

2.3.2. *Determination of optimal weight*

2.3.2.1. Analytic Hierarchy Process. Analytic Hierarchy Process (AHP) was proposed by Saaty (1990), which is a kind of decision analysis method that combines qualitative and quantitative analysis. Based on the scoring judgment matrix of the relative importance of the two indicators, which are then aggregated, the weights of each factor are finally calculated (Hoque et al., 2020; Zarei et al., 2021).

2.3.2.2. Entropy method. Entropy method is an objective method for determining weights, which could be used to quantify the amount of useful information in a given data. When the value of the evaluation object varies significantly, its entropy value is smaller, indicating that these data provide a large amount of useful information and the evaluation object should be given a higher weight (Meng, 1989; Qiu, 2002; Guo et al., 2021).

2.3.2.3. Criteria Importance Through Intercriteria Correlation. Criteria Importance Through Intercriteria Correlation (CRITIC) was developed by Diakoulaki et al. (1995). The CRITIC method is a comprehensive measure of the objective weight of the indicators based on the comparative strength of the evaluation indicators and the conflict between them (Jahan et al., 2012; Chang et al., 2020).

2.3.2.4. Fuzzy Comprehensive Evaluation. Zadeh (1965) introduced fuzzy comprehensive evaluation (FCE), which transformed qualitative evaluation into quantitative evaluation based on the affiliation theory of fuzzy mathematics. The method could better solve the issues of fuzzy and difficult to quantify, and is suitable for various non-deterministic problems (Wu et al., 2018; He et al., 2021).

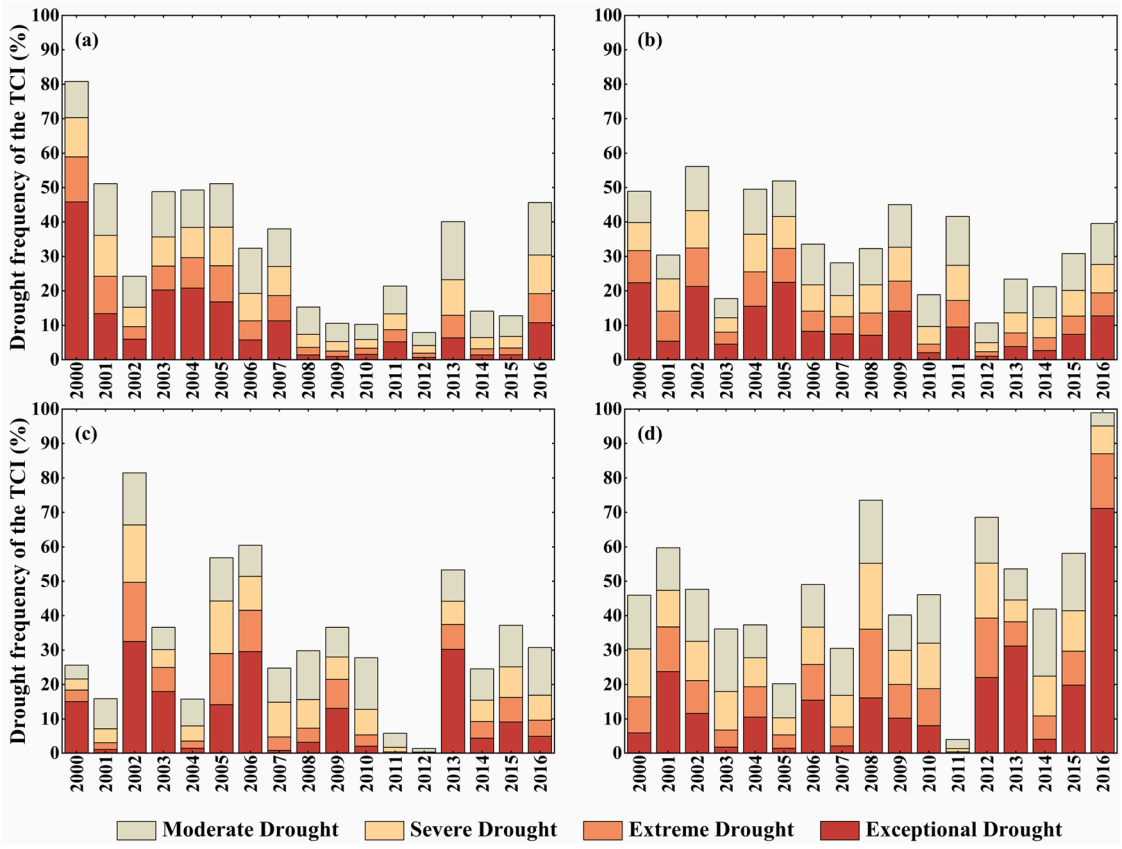

Fig. 8. Seasonal drought frequency of the Temperature Condition Index at monthly scale in the Wei River basin during the period 2000–2016. (a)Spring; (b)Summer; (c)Autumn; (d)Winter.

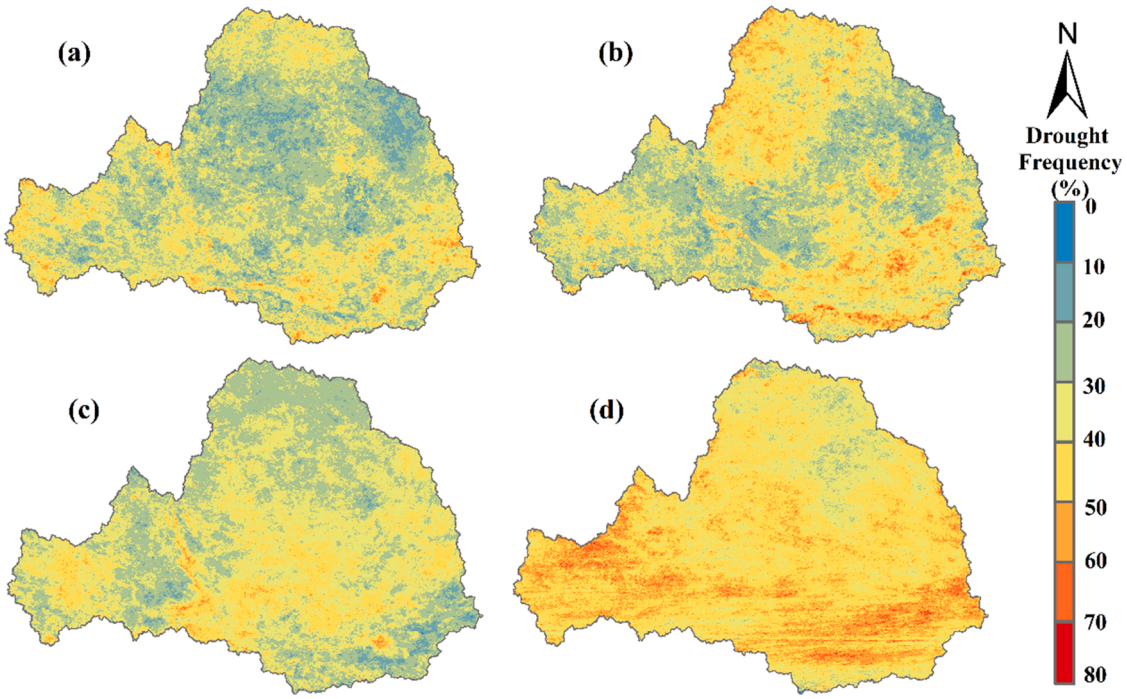

Fig. 9. Spatial distribution of seasonal drought frequency of the Temperature Condition Index in the Wei River basin during the period 2000–2016. (a)Spring; (b) Summer; (c)Autumn; (d)Winter.

Table 4
Optimal weights of SDCI for different methods.

Weight	AHP	Entropy	CRITIC	FCE
α	0.36	0.203	0.288	0.37
β	0.363	0.246	0.286	0.36
γ	0.277	0.551	0.426	0.27

3. Results and analysis

3.1. Applicability of the TRMM dataset in the WRB

In order to evaluate the applicability of the TRMM dataset in the WRB, the comparison between the temporal and spatial distribution of TRMM3B43 and rainfall data from 13 meteorological stations in the WRB during the period 2000–2016 were shown in Fig. 2. It can be seen from Fig. 2(a) and (b) that the R^2 between rainfall from 13 meteorological stations and TRMM3B43 were 0.83 and 0.65 at the monthly time scale and annual time scale, respectively. It proved that the TRMM3B43 dataset had well applicability in the WRB on both monthly and annual time scales. Moreover, a comparison of the spatial distribution of the TRMM3B43 dataset and 13 meteorological stations based on average annual precipitation was illustrated in Fig. 2(c). It was shown that the spatial distribution of the two kinds of datasets was substantially consistent. The annual precipitation was incremented from the north to the south, increasing from the west to the east. The TRMM3B43 dataset in the WRB showed an annual precipitation of 300–764 mm, while the rainfall from meteorological stations was from 386.7 to 840.9 mm. In general, the precipitation from the TRMM3B43 dataset could well reflect the spatial distribution of rainfall in the WRB, although its value was slightly lower than that of meteorological stations.

The variations of annual precipitation and annual precipitation anomaly percentage based on the TRMM3B43 dataset during the period 2000–2016 in the WRB were shown in Fig. 3. The average annual precipitation from 2000 to 2016 was 545.06 mm; the maximum value was 767.34 mm in 2003, higher than 40.78% of the average; the minimum precipitation reached 385.32 mm in 2016, lower than 29.31% of the average. Besides, the annual precipitation anomaly percentage was 17.7% and 16.51% in 2013 and 2011, respectively; and the annual precipitation anomaly percentage was − 14.62% and − 10.4% in 2008 and 2004, respectively. This indicated that the temporal variation of precipitation in the WRB was unstable, which is particularly prone to drought disasters.

3.2. Variations of drought identified by multiple indices

3.2.1. Drought variation based on the PCI

Based on TRMM3B43 precipitation data, the PCI was calculated in

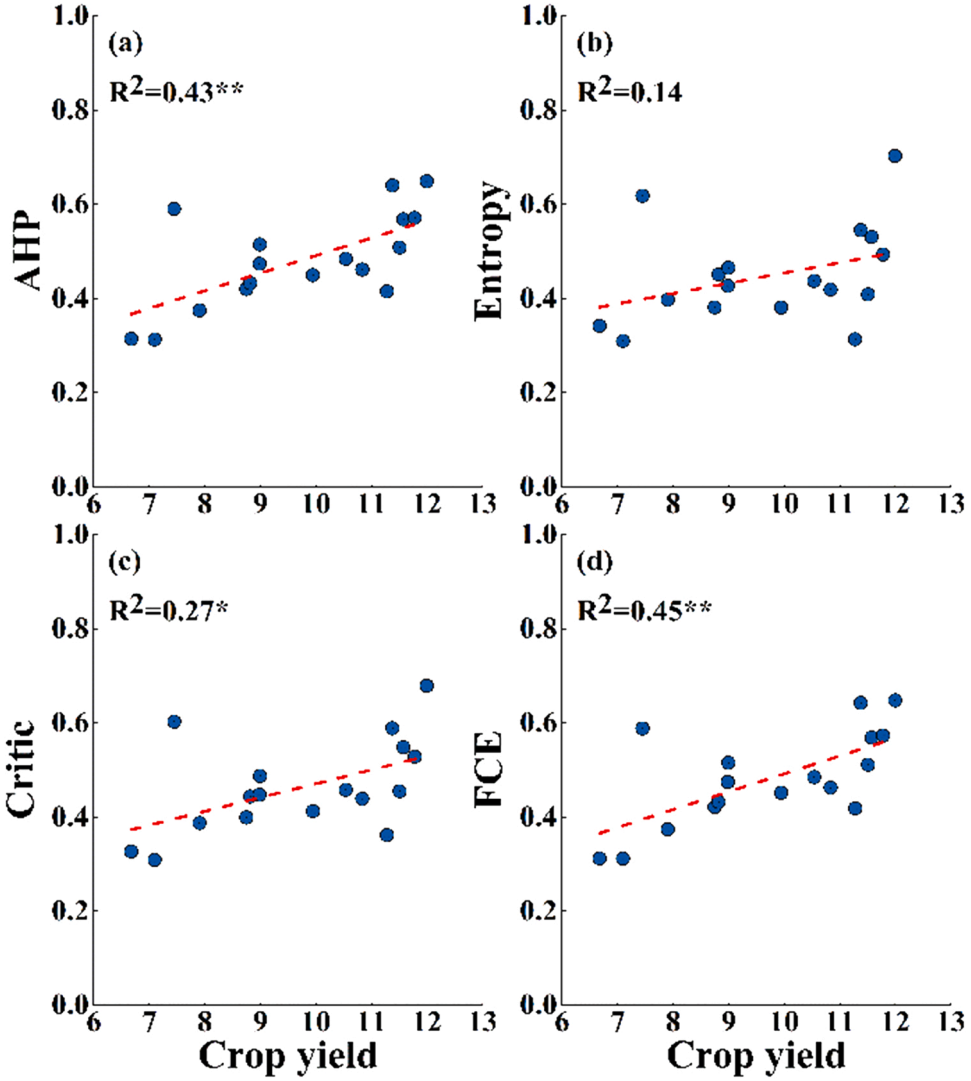

Fig. 10. The coefficient of determination (R^2) between the SDCI and CY under different weighting methods during the growing season from 2000 to 2016.

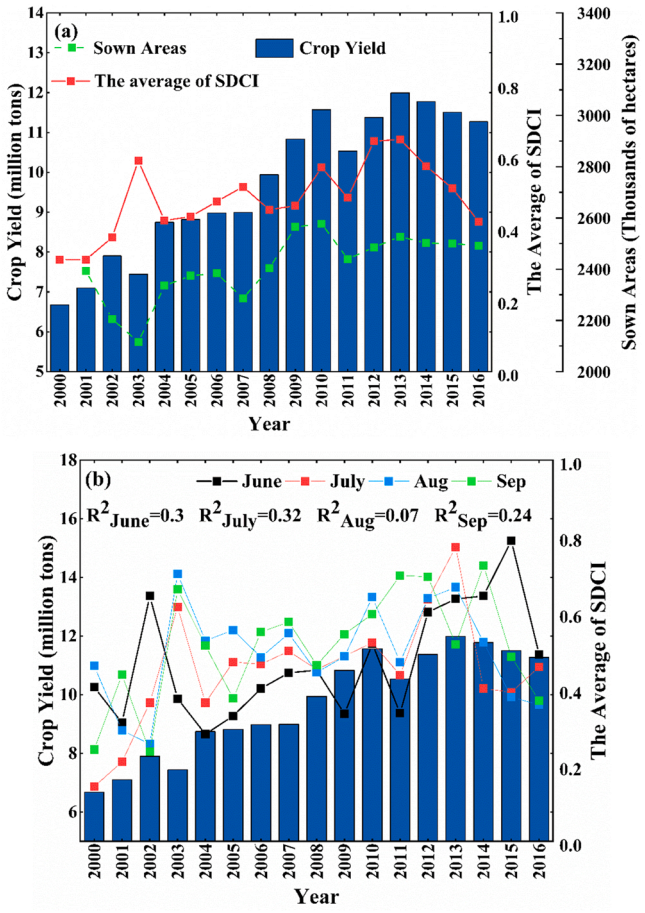

Fig. 11. Temporal variation of the Scaled Drought Condition Index for growing season in the Wei River basin during the period 2000–2016. (a) at annual scale; (b) at monthly scale.

the WRB for the period 2000–2016 (Fig. 4). The red and blue boxes indicate the negative and positive values of the percentage of precipitation anomalies, respectively. Except for the year 2003, all the mean values of PCI (PCI-mean) were less than 0.5, which meant that the WRB occurred different degrees of drought during the period 2000–2016. The distributions of the PCI value for the years 2000, 2005, and 2012 were relatively dispersed, while those for the years 2001, 2004, and 2015 were relatively concentrated.

The spatial distribution of the PCI in the WRB during the period 2000–2016 was presented in Fig. 5. Before the year 2010, the drought in the north of the WRB was heavier than that in the south, except in the years 2002 and 2007; After the year 2010, on the contrary, the drought in the south was heavier than that in the north. Except the year 2003, drought events with varying degrees often occurred in the central region of the basin.

3.2.2. *Drought variation based on the VCI*

Temporal variations and spatial distributions of the VCI in the WRB during the period 2000–2016 were shown in Fig. 6 and Fig. 7, respectively. It can be concluded from Fig. 6, the frequency of exceptional drought based on the VCI was 27.59% and 1.93% in the years 2000 and 2001, respectively. In all other years, the frequency of exceptional droughts was less than 0.1%, which could assume that no extreme drought events occurred in other years. The trend of the frequency of extreme drought based on the VCI was similarly to that for exceptional drought, 26.95% and 21.71% in the years 2000 and 2001, respectively. In all other years, the frequency of extreme droughts was almost less than 1%. The percentages of severe drought and moderate drought generally showed a trend of fluctuating downward.

It can be seen from Fig. 7 that the drought in the WRB identified by the VCI was more severe in the northern part in the years 2000 and 2001, and began to be mitigated in the year 2002, which was the positive effect of the national policy of returning farmland to the forest (grass) implemented around the year 1999, and ecological restoration projects have been carried out in the WRB, such as returning farmland to forests, closing mountains for forest cultivation, and protecting natural secondary forests. The implementation of these ecological restoration projects had caused sloping farmland, dry hilly gully region, and low to medium cover grassland, which were originally covered by sparse crops or grass, to be replaced by forest or grassland. The average VCI value in the WRB was relatively low with about 0.2 in the year 2000, as the period of tree growth was still short, the ecological restoration projects had not yet completely established; then the measures began to bear fruit and the overall situation of vegetation cover improved with an average VCI value of 0.3 in the year 2001.

In the years 2002 and 2003, the drought was relatively severe in the central region; in the years 2005–2008, the northern region experienced severe drought, which was more severe than that in other regions. After the year 2009, the severity of the drought had been mitigated across the basin. A moderate drought occurred in the year 2013 in the south-eastern region, which had been alleviated in the years 2014 and 2015, however, a moderate drought returned to hit the south-eastern and central-western regions.

3.2.3. *Drought variation based on the TCI*

The drought frequency based on the TCI at monthly interval in the WRB during the period 2000–2016 was illustrated in Fig. 8. In China, a year is divided into four seasons: spring (March-May), summer (June-August), autumn (September-November) and winter (December-February next year).

In terms of multi-year average seasonal drought frequency (moderate drought and above), winter had the highest frequency of drought (47.74%), followed by summer (34.11%), autumn (33.21%), and spring (32.58%). In spring, the frequency of moderate drought, severe drought, extreme drought, and exceptional drought all showed a downward trend with 2%/10 y, 3.2%/10 y, 4.3/10 y, and 14.6%/10 y, respectively. In summer, the frequency of severe drought, extreme drought, and exceptional drought all showed a downward trend; while moderate drought showed a slight upward trend (0.7%/10 y). As for exceptional drought, the frequency of occurrence was relatively high before the year 2005 and began to decline from the year 2006. In autumn, the frequency of severe drought, extreme drought, and exceptional drought all showed a downward trend; while moderate drought showed a slightly upward trend (0.9%/10 y). In winter, the frequencies of exceptional drought and extreme drought showed an upward trend; while severe drought and moderate drought showed a downward trend.

The spatial distributions of frequency of seasonal drought based on the TCI in the WRB during the period 2000–2016 were shown in Fig. 9. The frequency of spring drought was below 40% in most of the WRB, while that in the surrounding areas, such as the north, south, east, and west was relatively high, ranging between 40% and 60%. In summer, half of the WRB had a drought frequency of less than 40%, mainly in the central and western regions, while most of the southern and northern regions contributed a drought frequency between 40% and 60%. The frequency of droughts in autumn was the opposite of that in summer, with relatively low frequency in the south and north and relatively high frequency in the central WRB. The frequency of drought was relatively high in winter compared to other seasons. The frequency of winter drought in the northern, midwestern, and southern margins was below 40%, while that in the most region of the WRB, especially for the western, south-central regions, was between 40%– 60%.

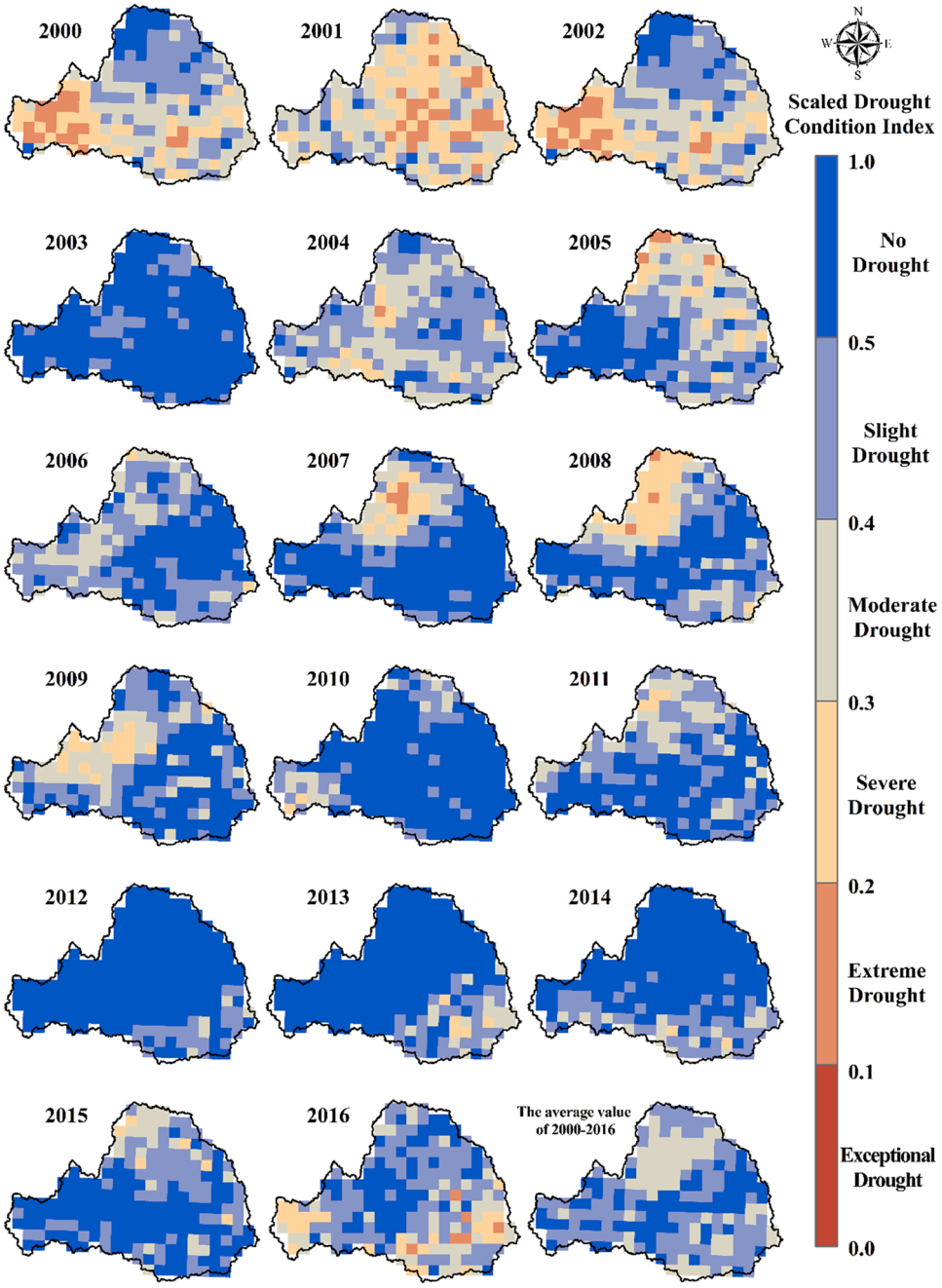

Fig. 12. Spatial distribution of the Scaled Drought Condition Index for growing season in the Wei River basin during the period 2000–2016.

3.3. Agricultural drought assessment by using the SDCI

3.3.1. Comparisons between crop yield and the SDCIs under different weights

To determine the suitable weights for the SDCI in the WRB, four different methods were used to obtain the weighting results using TCI, VCI and PCI data as inputs for June-September from 2000 to 2016. The optimal weights were shown in Table 4. In terms of these four results, the difference between the weights of the VCI and TCI was relatively small. The weights of the PCI were relatively larger than those of the TCI and VCI, except for the AHP and FCE methods.

To better assess the performance of SDCIs, the coefficient of determination (R^2) between the SDCI and CY calculated under different weighting methods during the growing season from 2000 to 2016 was illustrated in Fig. 10. In terms of CY dataset, the lack of data for Ningxia Hui Autonomous Region in 2000 may have some influence on the results. In Fig. 10, the R^2 between FCE-SDCI and CY was the highest with 0.45, while the R^2 for entropy-SDCI were the lowest with 0.14. Therefore, the weights of FCE were selected for the following SDCI calculation and analysis.

3.3.2. Spatiotemporal variations of the SDCI

Based on the calculation of the PCI, VCI, and TCI with the weights of FCE, the agricultural drought in the WRB for the period 2000–2016 was assessed by the SDCI, Fig. 11 showed the temporal variation of agricultural drought at annual and monthly scale.

As can be seen from Fig. 11(a), the variation of CY generally followed the changes in the SDCI value. The SDCI values exhibited a "W" fluctuation from 2003 to 2010 during the growing seasons. The VCI showed a slightly upward trend, while PCI demonstrated the opposite trend; The

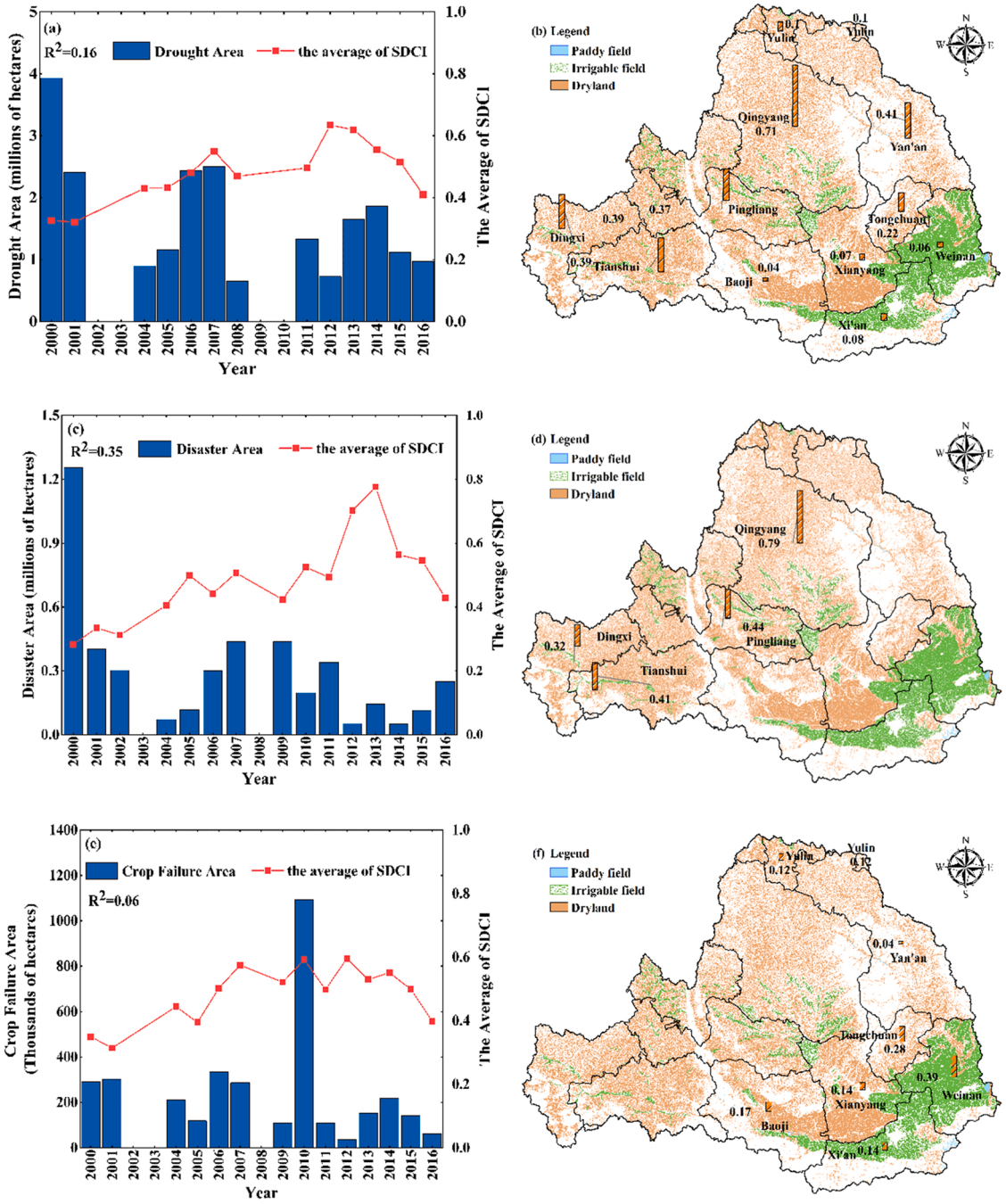

Fig. 13. R^2 between the Scaled Drought Condition Index with crop production from 2000 to 2016. (a) R^2 between the SDCI and drought area at the whole basin scale; (b) R^2 between the SDCI and drought area at municipal scale; (c) R^2 between the SDCI and disaster area at the whole basin scale; (d) R^2 between the SDCI and disaster area at municipal scale; (e) R^2 between the SDCI and crop failure area at the whole basin scale; (f) R^2 between the SDCI and crop failure area at municipal scale.

TCI also presented a "W" shape, and there was a turning point in the year of 2007. The changing trend of the SDCI was similar to that of the TCI, showing a "W" shape, which indicated that the SDCI comprehensively considers the drought situation on the basis of fully considering all factors, and the influence of temperature in this region was greater than that of precipitation. After 2008, the CY increased as the average of SDCI increased, and decreased as the average of SDCI decreased. However, for the same value of SDCI, there were some differences in the CY. For instance, the SDCI values for 2008 and 2009 were almost identical with 0.45 and 0.46 respectively, while CY were 10.83 million tons and 9.94 million tons, respectively, a difference of 0.89 million tons was mainly due to the difference in their sown areas of 125.16 thousand hectares. In addition, the SDCI value for 2002 was 0.37 with a moderate drought occurred, and CY was 7.9 million tons, while the SDCI value for 2003 was 0.59 with no drought happened, and CY was only 7.45 million tons. It also maybe on account of sown areas of 2205.35 thousand hectares in 2002 and 2115.99 thousand hectares in 2003, a reduction of 89.36 thousand hectares in the sown areas.

Temporal variation of the SDCI at the monthly scale was presented in Fig. 11(b). The SDCI values of the four months all showed an upward trend of fluctuation in different degrees, indicating that the drought degree of the WRB had decreased. The R^2 between monthly SDCI and CY had the highest value in July with 0.32, followed by June with 0.3, the lowest value in August with 0.07. Therefore, throughout the whole

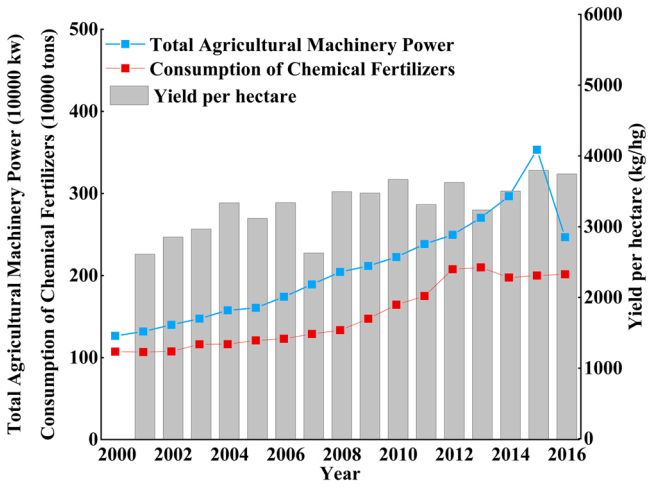

Fig. 14. The influence of agricultural modernization affecting agricultural drought in Shaanxi Province.

growing season, the beginning month of sown had a great influence on the CY.

The spatial distributions of the growing seasons SDCI in the WRB during the period 2000–2016 were shown in Fig. 12. It can be seen that droughts events occurred in most parts of the basin before 2002, and the severity of the drought reduced after 2003. A severe drought occurred in the northern part of the basin until 2008, after which it showed weakening and a shift from the northern to the southern part of the basin. Most areas of the basin experienced drought events in 2016.

3.3.3. *Utility of SDCI in drought disaster monitoring*

To better demonstrate the utility of the SDCI to assess agricultural drought in the WRB, the SDCI was also analyzed in comparison with the drought area, disaster area, and crop failure area. Areas where crop yield have been reduced by more than 10%, 30%, 80% due to drought are defined as drought area, disaster area, and crop failure area, respectively. The year of 2003 with extremely high precipitation was excluded from this analysis.

The drought area and SDCI values of Gansu Province and Shaanxi Province were compared and analyzed, the results were shown in Fig. 13 (a). Limited by data availability, R^2 between the SDCI and the drought area was 0.16, which did not show a good agreement, whereas the trends were consistent in some years. For example, the SDCI value first increased and then decreased from 2011 to 2014, while the CY value first decreased and then increased. In general, the SDCI values were less correlated with the drought area, and in turn the R^2 between SDCI values and the disaster area were selected for the following analysis.

The R^2 between the SDCI and the drought area at municipal scale of Gansu Province and Shaanxi Province in the WRB during the period 2000–2016 were presented in Fig. 13(b). The highest correlation coefficient is contributed by Qingyang (0.71), followed by Yan'an (0.41). Except for Xi'an (0.08), Xianyang (0.07), Weinan (0.06), Baoji (0.04) in the south and Yulin (0.1) in the north of the WRB, the R^2 of other regions were generally between 0.2 and 0.4. The results proved that the SDCI performed well in monitoring agricultural drought conditions in the western and central regions of the basin.

Comparative analysis of the disaster area and the SDCI values in Gansu Province and the results were shown in Fig. 13(c). The R^2 between the SDCI and areas affected was 0.35. From 2009–2016, the trend of changes in SDCI values and the disaster area remained largely consistent. The results showed that the SDCI values could well reflect the disaster area of the basin.

The R^2 between the SDCI values and the disaster area by each region in Gansu Province were shown in Fig. 13(d). It can be seen that the highest R^2 was produced by Qingyang (0.79), followed by Pingliang (0.44), Tianshui (0.41) and Dingxi (0.32). The drylands of Qingyang, Tianshui, Pingliang, and Dingxi accounted for 20.48%, 11.6%, 11.2%, and 8.86% of the total area of each region, respectively, which indicated that the SDCI index could well reflect the disaster area.

The average of SDCI across Shaanxi Province was calculated and then compared with the crop failure area from 2000 to 2016, which was shown in Fig. 13(e). A linear correlation between crop failure areas and the SDCI values was detected with a R^2 of 0.06. It can be seen that crop failure area reached a maximum of 10.93×10^5 hectares in 2010. According to news reports, in the winter of 2009 and early 2010, a drought occurred in Weinan of Shaanxi Province, with 70 consecutive days of no precipitation, and relative soil humidity in most fields fell below 50%, which was extremely harmful to summer crop growth. Therefore, the value of crop failure area in 2010 relatively higher was due to summer drought suffered by Weinan, rather than autumn drought.

Comparative analysis of crop failure areas and the SDCI values in Shaanxi Province and the results were shown in Fig. 13(f). Although Weinan produced the highest R^2 between crop failure area and the SDCI value (R^2 =0.39), the crop failure area was heavily influenced by the summer drought. In addition, the second highest R^2 was 0.28 from Tongchuan. Therefore, an analysis comparing the SDCI index with the drought area, disaster area and crop failure area showed that the SDCI can provide a good response not only to crop yield but also to the extent of agricultural disasters.

4. Discussion

4.1. *Determination of weights for variables in drought index*

The determination of the weight for each variable in drought index is very important for the accuracy of drought monitoring (Guo et al., 2019). Zhang and Jia (2013) proposed the Microwave Integrated Drought Index (MIDI), which is combined of PCI, SMCI and TCI, the weight is determined based on experimental weights. Huang et al. (2015) built an Integrated Drought Index combined runoff, soil moisture and precipitation using entropy method in the Yellow River Basin. An integrated drought condition index (IDCI) was developed by integrating SPEI-3, SMCI, and VCI by principal component analysis to determine the weights in Inner Mongolia China (Shen et al., 2019). In this study, four different methods were used to determine the weight, and the weight determined by comparison with crop yield not only makes up for the limitations of a single method, but also better reflects the agricultural drought rather than meteorological drought.

4.2. *Suitability of the SDCI for indicating agricultural drought*

The SDCI was based on precipitation, temperature, and vegetation data, including the impact of temperature changing rate, a lag time of agricultural drought responding to meteorological drought (3 months), comprehensive information regarding vegetation growth (Cao et al., 2022), which is suitable for identification and monitoring of agricultural drought.

The WRB is characterized as decreasing precipitation and increasing average air temperature at monthly scale (Huang et al., 2016). The SDCI value showed a small inflection point in the year of 2007, which was consistent with the change of temperature, while precipitation did not change significantly, indicating that the impact of temperature on SDCI was greater than precipitation. The finding is consistent with previous studies confirming that the influence of temperature on vegetation was greater than precipitation (Liu and Menzel, 2016). Furthermore, the growing season of corn is from June to September, which is consistent with the conclusion proposed by Dai et al. (2022) that PET and temperature are main influencing factor of drought propagation in summer.

The SDCI value showed in a "W" shape from 2003 to 2010 and it demonstrated that the WRB presented a transition from wet to dry, and then from dry to wet, which is consistent with the results of MIDI based

on Precipitation Anomaly Percentage, Runoff Anomaly Percentage, Standardized Precipitation Index with 6-month aggregation time step and Modified Palmer Drought Severity Index (Chang et al., 2016). The frequency of droughts was generally greater in the north than that in the south, and higher in the west than that in the east based on the SDCI, which is consistent with the finding of Yang et al. (2018) based on a nonlinear multi-variate drought index (NMDI).

4.3. The influence of agricultural modernization affecting agricultural drought

Agricultural modernization can effectively alleviate the impact of drought on people's life, it is essential to consider agricultural modernization factors for assessing the agricultural drought (Qin et al., 2015; Yang et al., 2018). To reduce the impact of agricultural drought, improving breeding, apply chemical fertilizers, increase the use of machinery and supplement farmland irrigation can be implemented in agricultural production (Wu et al., 2020). In order to better show the impact of agricultural modernization, Total Agricultural Machinery Power, Consumption of Chemical Fertilizers and yield per hectare of Shaanxi Province during the period 2000–2016 were shown in Fig. 14.

As observed in Fig. 14, the value of Total Agricultural Machinery Power firstly increased and then began to decrease at the year of 2015. The Total Agricultural Machinery Power is divided into three stages: "fluctuating upward (2003–2009) - stable forward (2010–2014) - beginning to decline (after 2015)" (Yang et al., 2020). During the Eleventh Five-Year Plan and the Twelfth Five-Year Plan, government vigorously promoted rural social and economic construction, raised the overall agricultural production capacity, and accelerated the process of agricultural modernization. The total power of agricultural machinery only declined in 2016, mainly because the insured amount of small agricultural machinery decreased (i.e. small tractors, small tractors towing farm machinery) according to the statistics data from Nation Bureau of Statistics.

The temporal variation of Consumption of Chemical Fertilizers showed firstly upward and then downward trend and the turning point at the year of 2013. In 2012, The People's Government of Shaanxi Province issued a three-year action to prevent and control water pollution in the WRB to reduce unreasonable fertilization and agricultural non-point source pollution (Shaanxi Provincial People's Government, 2012). Furthermore, The People's Government of Shaanxi Province issued a notice on a three-year action plan (2015–2017) to consolidate and improve the prevention and control of water pollution in the WRB (Shaanxi Provincial People's Government, 2015). It is expected to reduce agricultural non-point source pollution and other problems in the basin.

The yield per hectare displayed an upward trend of fluctuation. In 2004, the value increased greatly because of the change of corn planting varieties in Guanzhong Plain (Lei et al., 2012). Before 2004, the corn planted in the west of Guanzhong Plain was a single hybrid with high quality and high yield. At the year of 2004, the single hybrids with high yield and multi resistance was planted. The value in the year of 2007 was lower maybe due to the rapid reduction of planting area.

Therefore, it can be reasonably concluded that the variations of agricultural drought were caused by both climate change and human activities (Huang et al., 2015). In the case of the SDCI combining three factors, the impact of human activities may account for a certain proportion (Zhang et al., 2019). The impact of human activities and climate change on agricultural drought can be further considered separately in the future.

5. Conclusions

In this study, the SDCI was used by determining variable weights based on three remote sensing components (PCI, VCI, and TCI) to assess the agricultural drought in the Wei River basin of China from 2000 to 2016. The performance of SDCI was evaluated based on crop yield compared with four kinds of weights determination methods. And then, drought area, disaster area and crop failure area were used to validate the results of the agricultural drought assessment. The main conclusions are summarized as follows:

A comparison of precipitation from TRMM3B43 and meteorological gauging stations showed that the TRMM3B43 could accurately characterize the precipitation across the WRB at annual and monthly scales, whereas the precipitation was underestimated. Based on the TRMM3B43 dataset, the maximum precipitation reached 767.34 mm in 2003 and the minimum reached 385.32 mm in 2016. The precipitation in the south of the WRB was greater than that in the north, while that in the east was greater than the west.

The arid area of the WRB shifted from the north to the south based on the PCI analysis, and the arid area showed a decreasing trend after 2008. The drought frequency and arid area both showed a decreasing trend indicated by the VCI, and the arid area similarly shifted from the north to the south. The drought frequency showed a downward trend at the seasonal scale calculated by the TCI.

The SDCI correlates well with crop yield based on FCE with the R^2 of 0.45. The temporal variation of the SDCI value showed a "W" fluctuation from 2003 to 2010. Comparing with the drought area, disaster area, and crop failure area, it indicated that the SDCI provides a good assessment of the severity of agricultural drought in the Wei River basin of China.

In conclusion, the SDCI is applicable to the evaluation of agricultural drought in the Wei River Basin of China and provides strong support for agricultural disaster prevention, disaster risk reduction and disaster loss reduction.

Declaration of Competing Interest

The authors declare that they have no known competing financial interests or personal relationships that could have appeared to influence the work reported in this paper.

Data Availability

I have shared my data in the manuscript.

Acknowledgments

This study is jointly supported by National Key Research and Development Program of China (Grant No. 2021YFC3201104, 2021YFC3201502), Joint Open Research Fund Program of State key Laboratory of Hydro Science and Engineering and Tsinghua – Ningxia Yinchuan Joint Institute of Internet of Waters on Digital Water Governance (Grant No. sklhse-2022-Iow07), Open Project of Key Laboratory of Soil and Water Conservation on Loess Plateau of Ministry of Water Resources (Grant No. WSCLP202102).

References

Aghakouchak, A., Farahmand, A., Melton, F.S., et al., 2015. Remote sensing of drought: progress, challenges and opportunities. Rev. Geophys. 53 (2), 452–480. https://doi.org/10.1002/2014RG000456.

Barker, L., Hannaford, J., Chiverton, A., et al., 2015. From meteorological to hydrological drought using standardised indicators. Hydrol. Earth. Syst. Sci. 20 (6), 2483–2505. https://doi.org/10.5194/hess-20-2483-2016.

Beguería, S., Vicente-Serrano, S.M., Reig, F., et al., 2014. Standardized precipitation evapotranspiration index (SPEI) revisited: parameter fitting, evapotranspiration models, tools, datasets and drought monitoring. Int. J. Clim. 34 (10), 3001–3023. https://doi.org/10.1002/joc.3887.

Cao, S.P., Zhang, L.F., He, L., et al., 2022. Effects and contributions of meteorological drought on agricultural drought under different climatic zones and vegetation types in Northwest China. Sci. Total. Environ. 821, 153270. https://doi.org/10.1016/j.scitotenv.2022.153270.

Chang, J.X., Li, Y.Y., Wang, Y.M., et al., 2016. Copula-based drought risk assessment combined with an integrated index in the Wei River Basin, China. J. Hydrol. 540, 824–834. https://doi.org/10.1016/j.jhydrol.2016.06.064.

Chang, Y.J., Zhu, D.M., 2020. Urban water security of China's municipalities: comparison, features and challenges. . J. Hydrol. 587, 125023 https://doi.org/10.1016/j.jhydrol.2020.125023.
Chen, H.P., Sun, J.Q., 2015. Changes in drought characteristics over China using the standardized precipitation evapotranspiration index. J. Clim. 28 (13), 5430–5447. https://doi.org/10.1175/JCLI-D-14-00707.1.
Chen, S.B., Chen, Y.W., Chen, J.Y., et al., 2020. Retrieval of cotton plant water content by UAV-based vegetation supply water index (VSWI). Int. J. Remote. Sens. 41 (11), 4389–4407. https://doi.org/10.1080/01431161.2020.1718234.
Chu, H.S., Venevsky, S., Wu, C., et al., 2019. NDVI-based vegetation dynamics and its response to climate changes at Amur-Heilongjiang River Basin from 1982 to 2015. Sci. Total. Environ. 650, 2051–2062. https://doi.org/10.1016/j.scitotenv.2018.09.115.
Cruz-Roa, A.F., Olaya-Marín, E.J., Barrios, M.I., 2017. Ground and satellite based assessment of meteorological droughts: the Coello river basin case study. Int. J. Appl. Earth Obs. Geoinf. 62, 114–121. https://doi.org/10.1016/j.jag.2017.06.005.
Dai, M., Huang, S.Z., Huang, Q., et al., 2022. Propagation characteristics and mechanism from meteorological to agricultural drought in various seasons. J. Hydrol. 610, 127897. https://doi.org/10.1016/j.jhydrol.2022.127897.
Diakoulaki, D., Mavrotas, G., Papayannakis, L., 1995. Determing objective weights in multiple criteria problems: The CRITIC method. Comput. Oper. Res. 22 (7), 763–770. https://doi.org/10.1016/0305-0548(94)00059-h.
Ding, L., Mao, R.F., Guo, X., et al., 2019. Microplastics in surface waters and sediments of the Wei River, in the northwest of China. Sci. Total Environ. 667, 427–434. https://doi.org/10.1016/j.scitotenv.2019.02.332.
Faiz, M.A., Liu, D., Fu, Q., et al., 2020. Assessment of dryness conditions according to transitional ecosystem patterns in an extremely cold region of China. J. Clean. Prod. 255, 120348 https://doi.org/10.1016/j.jclepro.2020.120348.
Fang, W., Huang, S.Z., Huang, Q., et al., 2020. Identifying drought propagation by simultaneously considering linear and nonlinear dependence in the Wei River basin of the Loess Plateau, China. J. Hydrol. 591, 125287 https://doi.org/10.1016/j.jhydrol.2020.125287.
Gao, P., Geissen, V., Ritsema, C.J., 2012. Impact of climate change and anthropogenic activities on stream flow and sediment discharge in the Wei River basin, China. Hydrol. Earth Syst. Sci. Discuss. 9, 3933–3959. https://doi.org/10.5194/hessd-9-3933-2012.
Gazol, A., Camarero, J.J., Vicente-Serrano, M.S., et al., 2018. Forest resilience to drought varies across biomes. Glob. Change Biol. 24, 2143–2158. https://doi.org/10.1111/gcb.14082.
Guo, H., Bao, A.M., Liu, T., et al., 2019. Determining variable weights for an optimal scaled drought condition index (OSDCI): evaluation in central Asia. Remote. Sens. Environ. 231, 111220 https://doi.org/10.1016/j.rse.2019.111220.
Guo, H.P., Chen, J., Pan, C.L., 2021. Assessment on agricultural drought vulnerability and spatial heterogeneity study in China. Int. J. Environ. Res. Public Health. 18, 4449. https://doi.org/10.3390/ijerph18094449.
Guo, Y., Huang, S.Z., Huang, Q., et al., 2020. Propagation thresholds of meteorological drought for triggering hydrological at various levels. Sci. Total. Environ. 712, 136502 https://doi.org/10.1016/j.scitotenv.2020.136502.
Hayes, M., Svoboda, M., Wilhite, D., 1999. Monitoring the 1996 drought using the Standardized Precipitation Index. Bull. Am. Meteorol. Soc. 80 (3), 429–438. https://doi.org/10.1175/1520-0477(1999)080<0429:MTDUTS>2.0;CO2.
He, L., Du, Y., Wu, S., et al., 2021. Evaluation of the agricultural water resource carrying capacity and optimization of a planting-raising structure. Agric. Water Manag. 243, 106456 https://doi.org/10.1016/j.agwat.2020.106456.
Hoque, A.A., Pradhan, B., Ahmed, N., 2020. Assessing drought vulnerability using geospatial techniques in northwestern part of Bangladesh. Sci. Total. Environ. 705, 135957 https://doi.org/10.1016/j.scitotenv.2019.135957.
Hu, X.B., Ren, H.Z., Tansey, K., et al., 2019. Agricultural drought monitoring using European Space Agency Sentinel 3A land surface temperature and normalized difference vegetation index imageries. Agric. Meteor. 279, 1–9. https://doi.org/10.1016/j.agrformet.2019.107707.
Huang, S., Chang, J., Huang, Q., et al., 2014. Spatio-temporal changes and frequency analysis of drought in the Wei River basin, China. Water Res. Manag. 28 (10), 3095–3110. https://doi.org/10.1007/s11269-014-0657-4.
Huang, S., Chang, J., Leng, G., et al., 2015. Integrated index for drought assessment based on variable fuzzy set theory: a case study in the Yellow River basin, China. J. Hydrol. 527, 608–618. https://doi.org/10.1016/j.jhydrol.2015.05.032.
Huang, S., Huang, Q., Leng, G., et al., 2017. Variations in annual water-energy balance and their correlations with vegetation and soil moisture dynamics: a case study in the Wei River basin, China. J. Hydrol. 546, 515–525. https://doi.org/10.1016/j.jhydrol.2016.12.060.
Huang, S.Z., Huang, Q., Chang, J.X., et al., 2015. The response of agricultural drought to meteorological drought and the influencing factors: a case study in the Wei River Basin, China. Agric. Water Manag. 159, 45–54. https://doi.org/10.1016/j.agwat.2015.05.023.
Huang, S.Z., Huang, Q., Zhang, H.B., et al., 2016. Spatio-temporal changes in precipitation, temperature and their possibly changing relationship: a case study in the Wei River Basin, China. Int. J. Climatol. 36, 1160–1169. https://doi.org/10.1002/joc.4409.
Huang, S.Z., Li, P., Huang, Q., et al., 2017. The propagation from meteorological to hydrological drought and its potential influence factors. J. Hydrol. 547, 184–195. https://doi.org/10.1016/j.jhydrol.2017.01.041.
Jahan, A., Mustapha, F., Sapuan, S.M., et al., 2012. A framework for weighting of criteria in ranking stage of material selection process. Int. J. Adv. Manuf. Technol. 58 (1–4), 411–420. https://doi.org/10.1007/s00170-011-3366-7.
Jehanzaib, M., Shah, S.A., Yoo, J., et al., 2020. Investing the impacts of climate change and human activities on hydrological using non-stationary approaches. J. Hydrol. 588, 125052 https://doi.org/10.1016/j.jhydrol.2020.125052.
Kalisa, W., Zhang, J.H., Igbawua, T., et al., 2020. Spatio-temporal analysis of drought and return periods over the East African region using Standardized Precipitation Index from 1920 to 2016. Agric. Water Manag. 237, 106195 https://doi.org/10.1016/j.agwat.2020.106195.
Kogan, F.N., 1995. Application of vegetation index and brightness temperature for drought detection. Adv. Space Res. 15 (11), 91–100. https://doi.org/10.1016/0273-1177(95)00079-T.
Kogan, F.N., 1995. Droughts of the late 1980s in the United States as derived from NOAA polar- orbiting satellite data. Bull. Am. Meteorol. Soc. 76 (5), 655–668. https://doi.org/10.1175/1520-0477(1995)076<0655:DOTLIT>2.0.CO;2.
Lai, C.G, Zhong, R.D., Wang, Z.L., et al., 2019. Monitoring hydrological drought using long-term satellite-based precipitation data. Sci. Total. Environ. 649, 1198–1208. https://doi.org/10.1016/j.scitotenv.2018.08.245.
Lei, X.L., Meng, Q.L., Zhang, Y.W., et al., 2012. History of corn variety renewal and evolution in central and western Shaanxi Province. China Seed Ind. 1, 13–15.
Lesk, C., Rowhani, P., Ramankutty, N., 2016. Influence of extreme weather disasters on global crop production. Nature. 529 (7584), 84–87. https://doi.org/10.1038/nature16467.
Li, P.Y., Qian, H., Howard, K.W.F., et al., 2015. Building a new and sustainable "Silk Road economic belt". Environ. Earth Sci. 74 (10), 7267–7270. https://doi.org/10.1007/s12665-015-4739-2.
Li, P.Y., Qian, H., Zhou, W.F., 2017. Finding harmony between the environment and humanity: an introduction to the thematic issue of the Silk Road. Environ. Earth Sci. 76 (3), 105. https://doi.org/10.1007/s12665-017-6428-9.
Liu, Q., Zhang, S., Zhang, H.R., et al., 2020. Monitoring drought using composite drought indices based on remote sensing. Sci. Total. Environ. 711, 134585 https://doi.org/10.1016/j.scitotenv.2019.134585.
Liu, S., Huang, S., Xie, Y., et al., 2018. Spatial-temporal changes of rainfall erosivity in the loess plateau, China: changing patterns, causes and implications. Catena. 166, 279–289. https://doi.org/10.1016/j.catena.2018.04.015.
Liu, Z., Menzel, L., 2016. Identifying long-term variations in vegetation and climatic variables and their scale-dependent relationships: a case study in Southwest Germany. Glob. Planet. Change. 147, 54–66. https://doi.org/10.1016/j.gloplacha.2016.10.019.
Mckee, T.B., Doedken, N.J., Kleist, J., 1993. The relationship of drought frequency and duration to time scales. In: Eight Conf. On Applied Climatology. Amer. Meteor. Soc, American, CA, pp. 179–184.
Meng, Q.S., 1989. Information theory. Xi'An Jiaotong University Press, Xi'An, pp.19–36.
Palmer, W.C., 1965. Meteorological Drought. Weather Bureau Washington, DC, USA. US Department of Commerce.
Park, S., Im, J., Jang, E., et al., 2016. Drought assessment and monitoring through blending of multi-sensor indices using machine learning approaches for different climate regions. Agric. Meteorol. 216, 157–169. https://doi.org/10.1016/j.agrformet.2015.10.011.
Park, S., Im, J., Park, S., et al., 2017. Drought monitoring using high resolution soil moisture through multi-sensor satellite data fusion over the Korean peninsula. Agric. Meteorol. 237, 257–269. https://doi.org/10.1016/j.agrformet.2017.02.022.
Potop, V., Štěpánek, P., Možný, M., et al., 2015. Performance of the standardised precipitation evapotranspiration index at various lags for agricultural drought risk assessment in the Czech Republic. Agric. Meteorol. 202, 26–38. https://doi.org/10.1016/j.agrformet.2014.11.022.
Qin, Y., Yang, D.W., Lei, H.M., et al., 2015. Comparative analysis of drought based on precipitation and soil moisture indices in Haihe basin of North China during the period of 1960–2010. J. Hydrol. 526, 55–67. https://doi.org/10.1016/j.jhydrol.2014.09.068.
Qiu, W.H., 2002. Management Decision and Applied Entropy. China Machine Press, Beijing, pp. 193–196.
Rhee, J., Im, J., Carbone, G.J., 2010. Monitoring agricultural drought for arid and humid regions using multi-sensor remote sensing data. Remote. Sens. Environ. 114, 2875–2887. https://doi.org/10.1016/j.rse.2010.07.005.
Saaty, T.L., 1990. How to make a decision: the analytic hierarchy process Thomas. Eur. J. Oper. Res. 48 (1), 9–26. https://doi.org/10.1007/978-1-4614-3597-6_1.
Sahoo, A.K., Sheffield, J., Pan, M., et al., 2015. Evaluation of the Tropical Rainfall Measuring Mission Multi-Satellite Precipitation Analysis (TMPA) for assessment of large-scale meteorological drought. Remote. Sens. Environ. 159, 181–193. https://doi.org/10.1016/j.rse.2014.11.032.
Sánchez, N., González-Zamora, Á., Piles, M., et al., 2016. A New Soil Moisture Agricultural Drought Index (SMADI) Integrating MODIS and SMOS products: a case of study over the iberian Peninsula. Remote Sens. 8 (4), 287. https://doi.org/10.3390/rs8040287.
Schubert, S.D., Stewart, R.E., Wang, H., et al., 2016. Global meteorological drought: a synthesis of current understanding with a focus on SST drivers of precipitation deficits. J. Clim. 29 (11), 3989–4019. https://doi.org/10.1175/JCLI-D-15-0452.1.
Shaanxi Provincial People's Government Office. Three-Year Action Plan for Consolidation and Improvement of Water Pollution Prevention and Control in the Wei River Basin (2015–2017). Shaanxi Province, Shaanxi Provincial People's Government 2015 (in Chinese).
Shaanxi Provincial People's Government Office. Three-Year Action Plan for the Prevention and Control of Water Pollution in the Wei River Basin (2012–2014). Shaanxi Province, Shaanxi Provincial People's Government, 2012 (in Chinese).
Sheffield, J., Wood, E., Roderick, M., 2012. Little change in global drought over the past 60 years. Nature. 491 (7424), 435–438. https://doi.org/10.1038/nature11575.

Shen, Z.X., Zhang, Q., Singh, V.P., 2019. Agricultural drought monitoring across Inner Mongolia China: model development spatiotemporal patterns and impacts. J. Hydrol. 571, 793–804. https://doi.org/10.1016/j.jhydrol.2019.02.028.

Sjoukje, Y.P., Sarah, F.K., Karin, V.D.W., et al., 2020. Regional differentiation in climate change induced drought trends in the Netherlands. Environ. Res. Lett. 15, 094081 https://doi.org/10.1088/1748-9326/ab97ca.

Sur, C.Y., Hur, J.W., Kyoungjun, K., et al., 2015. An evaluation of satellite-based drought indices on a regional scale. Int. J. Remote. Sens. 36 (22), 5593–5612. https://doi.org/10.1080/01431161.2015.1101653.

Trenberth, K., Dai, A., Van der Schrier, G., et al., 2014. Global warming and changes in drought. Nat. Clim. Change. 4, 17–22. https://doi.org/10.1038/nclimate2067.

Van Loon, A.F., Laaha, G., 2015. Hydrological drought severity explained by climate and catchment characteristics. J. Hydrol. 526, 3–14. https://doi.org/10.1016/j.jhydrol.2014.10.059.

Vicente-Serrano, S.M., Beguería, S., López-Moreno, J.I., 2010. A multiscale drought index sensitive to global warming: the standardized precipitation evapotranspiration index. J. Clim. 23 (7), 1696–1718. https://doi.org/10.1175/2009JCLI2909.1.

Wang, H.S., Vicente-serrano, S.M., Tao, F.L., et al., 2016. Monitoring winter wheat drought threat in Northern China using multiple climate-based drought indices and soil moisture during 2000-2013. Agric. Meteorol. 228, 1–12. https://doi.org/10.1016/j.agrformet.2016.06.004.

Wells, N., Goddard, S., Hayes, M.J., 2004. A self-calibrating Palmer drought severity index. J. Clim. 17 (12), 2335–2351. https://doi.org/10.1175/1520-0442(2004)017<2335: ASPDSI>2.0.CO; 2.

Wu, B.F., Ma, Z.H., Yan, N.N., 2020. Agricultural drought mitigating indices derived from the changes in drought characteristics. Remote. Sens. Environ. 244, 111813 https://doi.org/10.1016/j.rse.2020.111813.

Wu, D., Li, Z.H., Zhu, Y.C., et al., 2021. A new agricultural drought index for monitoring the water stress of winter wheat. Agric. Water Manag. 244, 106599 https://doi.org/10.1016/j.agwat.2020.106599.FF.

Wu, L., Su, X.L., Ma, X.Y., et al., 2018. Integrated modeling framework for evaluating and predicting the water resources carrying capacity in a continental river basin of Northwest China. J. Clean. Prod. 204, 366–369. https://doi.org/10.1016/j.jclepro.2018.08.319.

Wu, Z., Mao, Y., Li, X., et al., 2016. Exploring spatiotemporal relationships among meteorological, agricultural, and hydrological droughts in Southwest China. Stoch. Environ. Res. Risk Assess. 30, 1033–1044. https://doi.org/10.1007/s00477-015-1080-y.

Xu, P.P., Zhou, T., Zhao, X., et al., 2018. Diverse responses of different structured forest to drought in Southwest China through remotely sensed data. Int. J. Appl. Earth. Obs. Geoinf. 69, 217–225. https://doi.org/10.1016/j.jag.2018.03.009.

Yang, H., Rui, Y., Li, J.L., et al., 2020. Spatiotemporal characteristics of agricultural modernization level and obstacles in Shaanxi Province (in Chinese). Res. Sci. 42 (1), 172–183. https://doi.org/10.18402/resci.2020.01.17.

Yang, J., Chang, J.X., Wang, Y.M., et al., 2018. Comprehensive drought characteristics analysis based on a nonlinear multivariate drought index. J. Hydrol. 557, 651–667. https://doi.org/10.1016/j.jhydrol.2017.12.055.

Yang, S.Y., Meng, D., Gong, H.L., et al., 2018. Soil drought and vegetation response during 2001–2015 in North China based on GLDAS and MODIS data. Adv. Meteor. 1818727, 1–14. https://doi.org/10.1155/2018/1818727.

Yao, N., Li, N., Yang, D.Q., et al., 2018. Bias correction of precipitation data and its effects on aridity and drought assessment in China over 1961-2015. Sci. Total. Environ. 639, 1015–1027. https://doi.org/10.1016/j.scitotenv.2018.05.243.

Yuan, F., Ma, M., Ren, L., et al., 2016. Possible future climate change impacts on the hydrological drought events in the Weihe River basin. Adv. Meteorol. 2905198, 1–14. https://doi.org/10.1155/2016/2905198.

Zadeh, L.A., 1965. Fuzzy Sets. Inf. Control. 8, 338–353. https://doi.org/10.1016/S0019-9958(65)90241-X.

Zarei, A.R., Moghimi, M.M., Koohi, E., 2021. Sensitivity assessment to the occurrence of different types of droughts using GIS and AHP techniques. Water Res. Manag. 35, 3593–3615. doi: 10.1007/s11269-021-02906-3.

Zhang, A., Jia, G., 2013. Monitoring meteorological drought in semiarid regions using multi-sensor microwave remote sensing data. Remote. Sens. Environ. 134, 12–23. https://doi.org/10.1016/j.rse.2013.02.023.

Zhang, S.N., Wu, Y.P., Bellie, S., et al., 2019. Climate change-induced drought evolution over the past 50 years in the southern Chinese Loess Plateau. Environ. Modell. Softw. 122, 104519 https://doi.org/10.1016/j.envsoft.2019.104519.

Zhang, Y., Huang, S.Z., Huang, Q., et al., 2019. Assessment of drought evolution characteristics based on a nonparametric and trivariate integrated drought index. J. Hydrol. 579, 124230 https://doi.org/10.1016/j.jhydrol.2019.124230.

Zhang, Y., Chao, Y., Fan, R.R., et al., 2021. Spatial-temporal trends of rainfall erosivity and its implication for sustainable agricultural in the Wei River basin of China. Agric. Water Manag. 245, 106557 https://doi.org/10.1016/j.agwat.2020.106557.

Zhao, J., Huang, Q., Chang, J.X., et al., 2015. Analysis of temporal and spatial trends of hydro-climatic variables in the Wei River Basin. Environ. Res. 139, 55–64. https://doi.org/10.1016/j.envres.2014.12.028.

Zhao, R.X., Wang, H.X., Zhan, C.S., et al., 2020. Comparative analysis of probability distributions for the Standardized Precipitation Index and drought evolution in China during 1961-2015. Theor. Appl. Climatol. 139, 1363–1377. https://doi.org/10.1007/s00704-019-03050-0.

Zhao, T.B., Yatagai, A., 2014. Evaluation of TRMM 3B42 product using a new gauge-based analysis of daily precipitation over China. Int. J. Climatol. 34 (8), 2749–2762. https://doi.org/10.1002/joc.3872.

Zhong, R.D., Chen, X.H., Lai, C.G., et al., 2019. Drought monitoring utility of satellite-based precipitation products across mainland China. J. Hydrol. 568, 343–359. https://doi.org/10.1016/j.jhydrol.2018.10.072.

Zhu, Y., Huang, S., Chang, J., et al., 2017. Spatial–temporal changes in potential evaporation patterns based on the Cloud model and their possible causes. Stoch. Environ. Res. Risk A. 31, 2147–2158. https://doi.org/10.1007/s00477-016-1304-9.

Zuo, D.P., Cai, S.Y., , et al.Xu, Z.X., 2019. Assessment of meteorological and agricultural droughts using in-situ. Agric. Water Manag. 222, 125–138. https://doi.org/10.1016/j.agwat.2019.05.046.